NASA/CR–2010-216682

Intelligent Flexible Materials for Space Structures

Expandable Habitat Engineering Development Unit

Jon Hinkle, George Sharpe, John Lin, Cliff Wiley, and Richard Timmers
ILC Dover, Frederica, Delaware

March 2010

NASA STI Program . . . in Profile

Since its founding, NASA has been dedicated to the advancement of aeronautics and space science. The NASA scientific and technical information (STI) program plays a key part in helping NASA maintain this important role.

The NASA STI program operates under the auspices of the Agency Chief Information Officer. It collects, organizes, provides for archiving, and disseminates NASA's STI. The NASA STI program provides access to the NASA Aeronautics and Space Database and its public interface, the NASA Technical Report Server, thus providing one of the largest collections of aeronautical and space science STI in the world. Results are published in both non-NASA channels and by NASA in the NASA STI Report Series, which includes the following report types:

- TECHNICAL PUBLICATION. Reports of completed research or a major significant phase of research that present the results of NASA programs and include extensive data or theoretical analysis. Includes compilations of significant scientific and technical data and information deemed to be of continuing reference value. NASA counterpart of peer-reviewed formal professional papers, but having less stringent limitations on manuscript length and extent of graphic presentations.

- TECHNICAL MEMORANDUM. Scientific and technical findings that are preliminary or of specialized interest, e.g., quick release reports, working papers, and bibliographies that contain minimal annotation. Does not contain extensive analysis.

- CONTRACTOR REPORT. Scientific and technical findings by NASA-sponsored contractors and grantees.

- CONFERENCE PUBLICATION. Collected papers from scientific and technical conferences, symposia, seminars, or other meetings sponsored or co-sponsored by NASA.

- SPECIAL PUBLICATION. Scientific, technical, or historical information from NASA programs, projects, and missions, often concerned with subjects having substantial public interest.

- TECHNICAL TRANSLATION. English-language translations of foreign scientific and technical material pertinent to NASA's mission.

Specialized services also include creating custom thesauri, building customized databases, and organizing and publishing research results.

For more information about the NASA STI program, see the following:

- Access the NASA STI program home page at *http://www.sti.nasa.gov*

- E-mail your question via the Internet to help@sti.nasa.gov

- Fax your question to the NASA STI Help Desk at 443-757-5803

- Phone the NASA STI Help Desk at 443-757-5802

- Write to:
  NASA STI Help Desk
  NASA Center for AeroSpace Information
  7115 Standard Drive
  Hanover, MD 21076-1320

NASA/CR–2010-216682

Intelligent Flexible Materials for Space Structures

Expandable Habitat Engineering Development Unit

Jon Hinkle, George Sharpe, John Lin, Cliff Wiley, and Richard Timmers
ILC Dover, Frederica, Delaware

March 2010

TABLE OF CONTENTS

1   Overview

This report covers work performed by ILC Dover, LP (ILC) in the design and fabrication of the eXpandable Habitat Engineering Development Unit (X-Hab EDU). This task order (NNL05AA28C) consists of the design, component testing, fabrication, and deployment testing of the full scale habitat. The goal of the program is to evaluate the packing and deployment of a full scale habitat unit under expected loading conditions.

The work performed for this task was based on the previous Intelligent Flexible Materials (InFlex) task orders. The work was influenced in particular by the Phase I InFlex engineering mockup and the Antarctic extreme environment test unit as seen in Figure 1.1.

Figure 1.1. Phase I InFlex mockup and Antarctic habitat

Softgoods are high strength fabric systems that are flexible and lightweight and can be used in extreme environments. They are collapsible and can therefore be packed into a much smaller volume than they occupy during operation. Softgoods have been used as lightweight deployable structures in numerous applications since the beginning of space exploration. Examples include satellites, Extra-Vehicular Activity (EVA) space suits, and impact attenuation bags for the Mars Exploration Rovers. Softgoods inflatable technology was used in the Transhab structure which was deployed in vacuum at Johnson Space Center in 1998. These types of structures, as seen in Figure 1.2, have several critical benefits for space operations. The first is that softgoods are collapsible. This facilitates their transportation in small launch vehicles, reducing cost. The internal configuration of a launch vehicle can also be optimized by using softgoods that take advantage of voids left by other components. Additionally, flexible deployable structures are lower in total weight in comparison to rigid mechanical structures, directly contributing to reduced launch costs. Inflatable structures also have the inherent advantage of reduced system complexity and increased system reliability due to minimal mechanical components required for their deployment and function.

Figure 1.2. Softgood examples. *(EMU Suit, MER Airbags, Transhab)*

The design, analysis and manufacture of the expandable habitat EDU will enable the team to fully evaluate inflatable habitats and raise the Technology Readiness Level of an expandable habitat structure. The primary purpose of the EDU is to allow critical examination of packing, deployment, interfaces, and outfitting of the deployed structure. Laboratory testing and field operations will further mature the expandable habitat design and assist in resolving the engineering challenge of an outpost on the Moon. Figure 1.3 shows the overall dimensions of the X-Hab in the packed and deployed configurations. Figure 1.4 is a photograph of the deployed system during inflation testing at ILC.
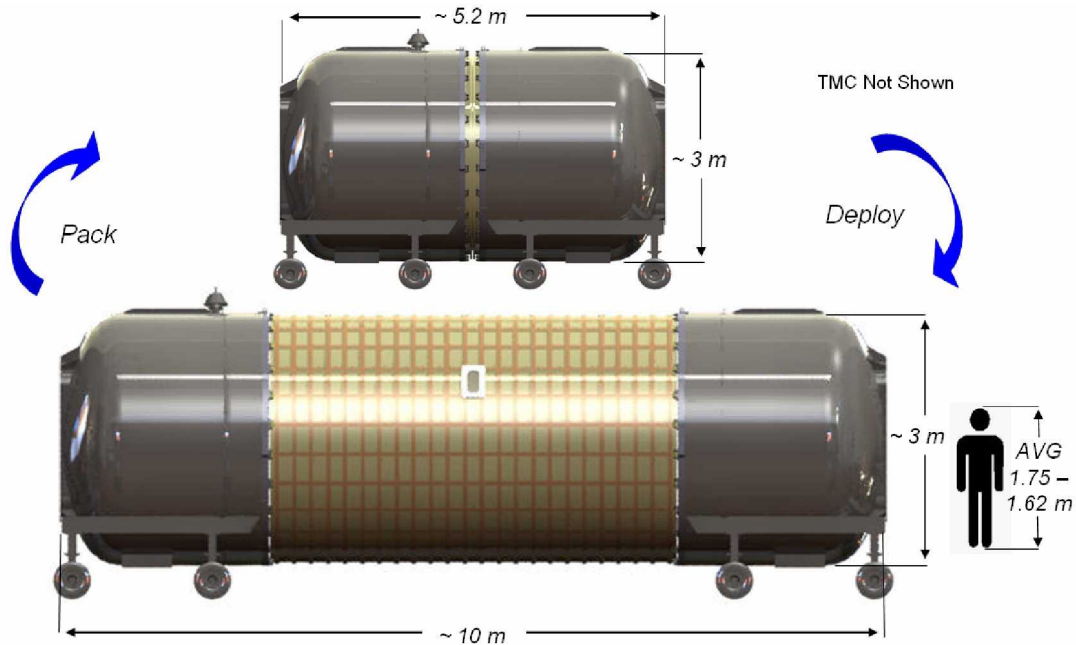
Figure 1.3. Packed and Deployed X-Hab. *Thermal Micrometeoroid Cover not shown and dimensions are only approximate baseline numbers.*

**Figure 1.4. Deployed system at ILC.**

2   Concept of Operations

An expandable habitat follows essentially the same mission plan for getting to and landing on the lunar surface as a rigid habitat. The main difference in the concept of operations is at the packing and deployment stages. Overarching requirements for a lunar habitat can be derived from the concept of operations.

The purpose of a lunar habitat is to provide a shirt sleeve environment where astronauts can live, sleep, and conduct experiments on the surface of the moon. The lunar outpost is envisioned as an incremental construction project. Various structures and rovers would be deployed by these first landings and connected together. The technology developed for the X-hab could be applied to a mobile unit or a stationary habitat. In either configuration, sufficient space is required for quarters, galley, experimental stations, and all the subsystems needed to survive in an extreme environment. An inflatable lunar habitat can offer a large habitable volume for a working research station while providing protection to the inhabitants.

For an expandable system, the softgoods must be secured in a packed state during launch, transit, and landing on the lunar surface. After landing, the launch ties can be released and the deployment initialized through inflation or by mechanical means. This deployment may be started immediately after touchdown or the habitat may remain in the packed state. Once the system is deployed and at full pressure, astronauts can enter via an airlock and outfit the habitat. The equipment can either come from a separate lander or be stored in the rigid endcaps. The structural integrity of the softgoods can be monitored throughout the transit and deployment events. Figure 2.1 is a pictorial depiction of a mission to land a habitat on the moon.

The EDU system is designed for testing on Earth at 9 psig. Testing is expected to be conducted at Langley Research Center (LaRC) and at White Sands, NM. The objective of the system is to critically evaluate the dynamics involved in deploying a large hybrid rigid / softgoods system. Secondary objectives include measuring leak rate and interior outfitting procedures.
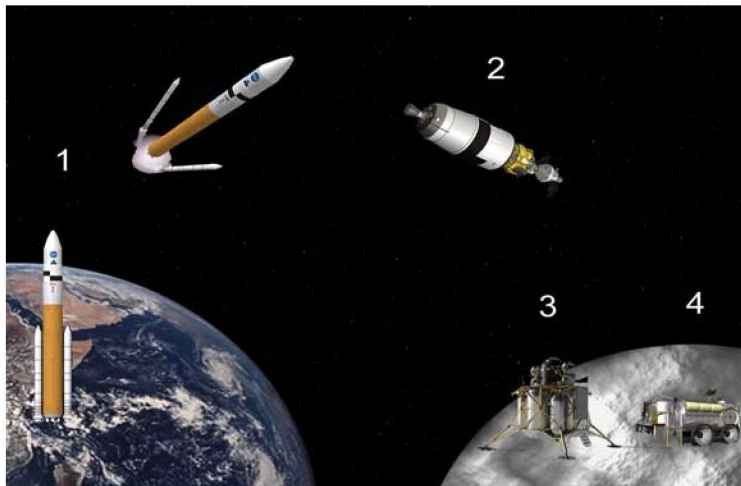
Figure 2.1. Habitat operations. *Launch of Ares V Cargo vehicle (1). Ares V positions lunar lander and continues toward the moon (2). Altair Lander module descends carrying the habitat (3). The outpost is setup on lunar surface (4).*

3 Design

The main objective of this program was to design an innovative and lightweight expandable habitat unit to demonstrate a unique system that offered mass savings and added volume over any other current system.

3.1 System Configuration

There are two basic configurations for a deployable cylindrical system. In one, a horizontal cylinder simulates a beam structure, where bending and deflection need to be taken into account. The other method is a vertical deployable architecture, which requires a larger diameter when compare to the horizontal architecture and the length is dictated by the desired height of the ceiling in order to achieve the same living volume as a horizontal system. The endcap of this system will need to be soft or hinge into the floor since the wall will need to have a freely expanding diameter. The circular walls also need to be interfaced with a cylindrical vehicle, resulting in two interfacing circles in a two dimensional frame. It is apparent that this interface will be more complicated than the configuration involving the horizontally deployed structure. Additionally, each configuration needs to be evaluated against mass and the operational scheme of the habitat. The mass of a system is directly related to the skin stress seen in the materials. The skin stress of an inflatable cylinder is proportional to the pressure and radius as seen in Equation 1. Therefore, a system that increases length over diameter will result in a mass optimized design. The functional height of the habitat is dictated by the astronauts' height. As a result, the horizontal cylinder is the desired option for this set of requirements.

$$\textit{Thin walled skin stress: } \sigma_h = \rho r \tag{1}$$

The deployment of the expandable section can be accomplished using several methods. The two basic approaches are a hinge design and a linear expansion, also known as an accordion deployment. The hinged method would be ideal for a vertical deployment by allowing the endcap to act as the floor. The linear or horizontal deployment is better suited for expanding a long cylinder shape. Two endcaps could then move apart allowing the center section to increase in volume without increasing the height. The linear expansion will therefore be the approach for the EDU.

3.2 Softgood Design

The habitat module is envisioned as being able to fit within the payload bay of the Ares V rocket and then expand on the lunar surface. Based on Lunar Architecture Team (LAT) studies, a goal of 3m diameter and an expanded length of 10m were set. The packed length of the softgoods had a maximum limit of 1m. Due to the uncertain nature of the packing process, the packed length and volume was not determined until the packing and deployment phase of the program. The X-hab is designed to carry an internal pressure load of 9 psig, while minimizing leakage, and protecting the inhabitants from the harsh lunar environment. Each layer in the laminate of flexible materials is optimized for a particular function.

3.2.1 Gas Retention Layer

The gas retention layer is the principal layer that maintains the atmosphere within the habitat. There are two primary methods for the leakage of gas: diffusion (permeation) and effusion. Diffusion is the leakage of gas through the material. Effusion is the leakage of gas

through large holes. These large holes can occur from internal abrasion, micrometeoroid events, or gaps in the bladder and hardware interface.

The bladder layer is separate in its function from any other layer. This method allows each layer to be optimized for its purpose. Abrasion and impact resistance in the bladder can be obtained via the use of a coated fabric. This material treatment gives the bladder strength while maintaining its diffusion characteristics. The fabric can be coated on both sides to further reduce diffusion while increasing durability. The double coating method also permits repairs from both sides and the application of cover tapes at seams. However, these double coating benefits must be measured against the increase in system mass and loss of some flexibility.

The bladder material is oversized, with respect to the restraint layer, to allow it to transfer pressure loads to the restraint system. The bladder will also have indexing pads to ensure that it is properly aligned with the rest of the softgoods. The indexing can be accomplished through a lightweight tab that is adhered or heat sealed to the bladder. The dimensionally oversized material will be relatively thin in its cross-section as it will not carry the skin stress loads due to pressure.

Redundancy could be added to the system by including a secondary or tertiary bladder layer. A second bladder would prevent gas from escaping in the case of a puncture. The second bladder would have to be separated by a spacer from the first system so that a puncture would not tear through both layers. Therefore, a second or third bladder may pose a significant mass penalty if a spacer or additional restraint system is required. Also a redundant bladder system offers problems if a repair is needed or if gas is trapped between layers.

The selection of materials for the fabrication of the EDU was based on the construction of spacesuits and work done by ILC on previous projects such as TransHab and InFlex. The material selection was also determined by the operational requirements and demonstration objectives for this expandable module. The primary layers of the expandable structure are: the gas retention layer (bladder), load bearing or structural layer (restraint), and the Thermal Micrometeoroid Cover (TMC) that provides thermal insulation and protection against radiation, dust and Micrometeoroids.

The material selected for the gas-retaining bladder of the habitat was a Fire Resistant Urethane Coated Vectran® fabric. The basecloth is composed of a 200 denier 50 x 50 plain weave construction that meets the minimum 400 pound per inch tensile requirement as determined by analysis. Vectran was selected as the base fiber as it has the proven capability to withstand the multiple flexural cycles that the habitat will experience. To render the basecloth air tight and fire retardant (FR) the fabric required additional processing.

In designing and specifying the final coated/laminated goods, it was noted that the type and amount of coating could significantly change the performance properties of the basecloth. Flexibility and weight were the major concerns among the properties affected. The more coating material added, the higher the fabric stiffness. As stiffness increases, flexibility decreases. Obviously, this could have a significant impact on the prototype performance. Therefore, ILC strove to minimize the effect that the additional FR processing conditions imposed on the basecloth while optimizing flexibility performance. These optimization efforts were accomplished in a collaborative effort with the fabric coater / laminator during the developmental stages of the bladder material development effort. Small developmental lab samples were -

8

fabricated and evaluated qualitatively and quantitatively for peel strength, seam strength, weight, and flame resistance.

3.2.2 Restraint Layer

The restraint layer carries the internal pressure load of the system. Several approaches can be taken to minimize the mass of this component while maintaining the desired safety factor. A safety factor of four was chosen due to its prevalent use in heritage inflatables and because this is a prototype unit. There is, for example a FAA safety factor requirement of 4 on all fabric airships. Also the lifetime performance of the newer high strength fiber webbings (such as Vectran) has not been studied in detail which recommends a higher safety factor until further research is performed. Hoop stress, as seen in Equation 1, is the driving factor dictating the construction technique of the habitat. In the Transhab module, the restraint system was a closed webbing net with a thin film bladder layer. A smaller habitat with lower stress could be designed to use only a coated fabric or a fabric with only hoop webbings. Figure 3.1 displays the trend of changing methods of construction with increasing stress. For the baseline EDU habitat diameter, the open webbing net offers a reduced mass system.

The open webbing net uses a combination of a webbing restraint and a coated fabric to carry the loading imposed by the 9 psi pressure load. The axial and hoop webbing net is designed to carry the entire loading condition, while the coated fabric handles the pressure loading in between the webbings. These fabric lobes bulge out between the crossovers and transfer the load to the webbings. The baseline material for both the webbing and the restraint fabric is Vectran. Vectran has several properties that make it an ideal choice for a lunar habitat. The most critical is its' high strength-to-weight ratio. In addition it retains its' strength during crease cycling and thermal exposure, and has excellent damage and abrasion resistance.
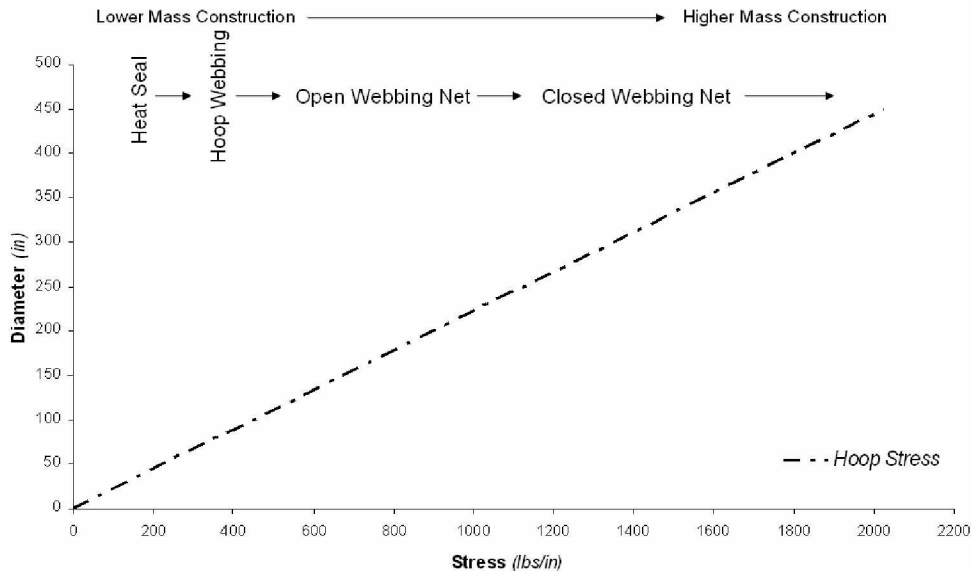
Figure 3.1. Habitat construction techniques

The open webbing net construction was based on the loading expected in the fabric. At the design radius of 59 inches (corresponding to the axial webbings) the expected loading in the fabric is 531 lbs/in. It is extremely difficult to estimate the load sharing between the fabric and the

webbing; therefore, the fabric is oversized to ensure that the webbing takes the entire pressure load. This allows the fabric to only see the loading in between the webbings, resulting in a 'fabric lobe' as seen in Figure 3.2. Based on these assumptions and a desired safety factor of 4, two Vectran webbings were selected for the final configurations; a 12k (12,000 lbf Ultimate Tensile Strength) and 24k (24,000 lbf UTS) webbing. The 12k and 24k Vectran webbing were readily available and any webbing with a lower UTS than 12k would begin to produce a webbing net design. The 24k webbing was chosen for this design as it decreased the amount of required interface hardware by reducing the total number of webbings (each taking a higher load). A model of the fabric lobe is shown in Figure 3.2 while an image of the indexing used on the habitat is shown Figure 3.3.
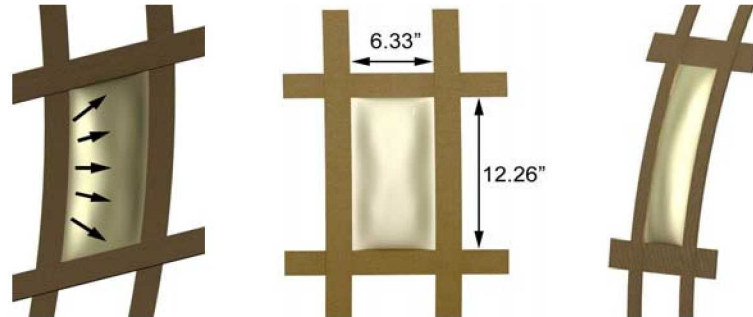
Figure 3.2. Fabric lobe
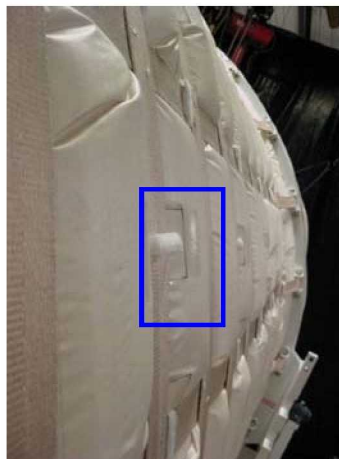
Figure 3.3. Indexing tabs for restraint fabric to webbing connections

3.2.3 *Thermal Micrometeoroid Cover*

The TMC provides protection to the habitat from the dangers of the lunar surface environment. The outer fabric provides radiation reflectance and puncture resistance from external cuts that may occur during Extra Vehicular Activity (EVA) or during transit. The multi layer insulation (MLI) is five to twenty or more layers of film for thermal insulation with a spacer to reduce conductive heat transfer. The Micro Meteoroid and Orbital Debris (MMOD) layer provides protection from high velocity particles. The purpose of this layer is to break apart the object and then have the foam absorb the vapor. Additional radiation protection could be provided by water or other materials with high hydrogen content.

The materials chosen for the TMC are based on simulating the physical characteristics of a true, space-rated Thermal Micrometeoroid Cover, and also on providing appropriate Earth

10

environment protection. The TMC material ply-up is designed to match the thickness and consistency of a true TMC to accurately model how a flexible TMC affects a deployable habitat during packing and deployment. Additionally, the TMC also provides flame resistance and protection from UV light for the flexible section of the habitat. The final material ply-up is shown in Figure 3.4.
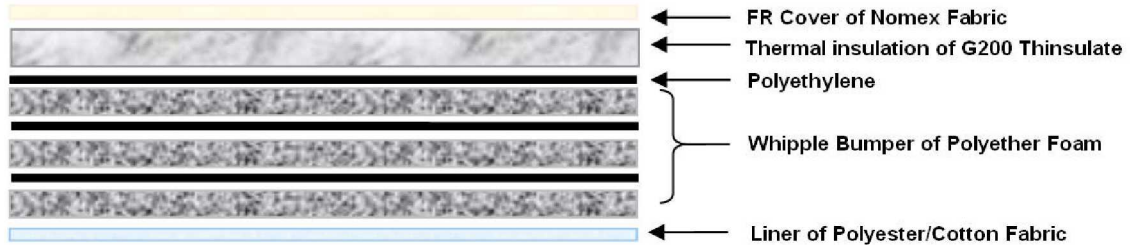
Figure 3.4. TMC final ply-up

The outer layer is composed of Nomex fabric which protects the exterior of the habitat from fire and handling damage. The next layer is a blanket of Thinsulate, to add some thermal insulation while also providing a realistic thickness to the ply-up. The next layer, polyethylene, is a UV blocker that keeps the UV-sensitive Vectran bladder and webbing from degrading. Three layers of 1/2 inch polyether foam simulate a Whipple Bumper of MLI. The innermost layer is a polyester lining fabric to aid in smooth deployment of the TMC. The total thickness for the representative TMC is approximately 2 inches.

The TMC is designed and patterned to be a cylinder, rather than a flat blanket wrapped around the habitat. The inside and outside layers have different circumferences due to the thickness of the TMC. In order to avoid the wrinkles and folds this would cause, the TMC is patterned to act like a sleeve over the habitat and should not interfere with the deployment or operations. For integration, the TMC will be strapped onto both endcaps and laced to itself. The lacing section is offset from the centerline of the habitat to provide access to the d-rings and lacing panel. Additionally, a Nomex lacing cover is included and the cord used for lacing is also Nomex. The entire surface of the TMC, as well as twelve inches inside of every opening, is blanketed with Nomex fabric. A cut through is provided on each side for the windows.

3.3   Hardware Interface

The hardware interface is the connection between the hardware and the softgoods. As the EDU is a test bed, a generic interface ring was designed that could be interchanged with multiple endcaps and handle the loading of several deployment scenarios. In a flight system, any interface between hardware and softgoods would be integral to the design and would be optimized for that specific system.

3.3.1   Webbing Bracket

The axial webbings are terminated at clevis pins on brackets attached to the ring. Webbing and sling manufacturers commonly use this approach due to it reducing abrasion and high stress pinch points on the webbing. It is also ideal for deployment as it allows the webbing to freely rotate. The lengths of the webbings are an important factor, as variations in length will affect the load distribution during and after inflation of the EDU. The bracket will have the option of shims on the backside to ensure that the webbing length can be tweaked to maintain the design length during the final integration. The webbing brackets will bolt directly onto the interface rings. The webbing bracket interface can be seen in Figure 3.5.

3.3.2   Interface Ring

Figure 3.5 details the interface between the softgoods and the hard endcaps. A standard method which is often utilized for a variety of sealing applications is the O-Ring. An example of a comparable O-Ring system can be seen in a large vacuum chamber. A groove is machined into the bulkhead and a clamp ring compresses the O-Ring placed along the channel. This clamp could be machined in several overlapping pieces and bolted behind the seal. For added leak resistance, a secondary or tertiary O-Ring could be installed behind the primary seal. Due to cost considerations, the outermost O-Ring groove was not included in the final configuration. The coated fabric is terminated into a 'deadman' and a urethane flange is compressed between the clamp ring and the O-Rings.
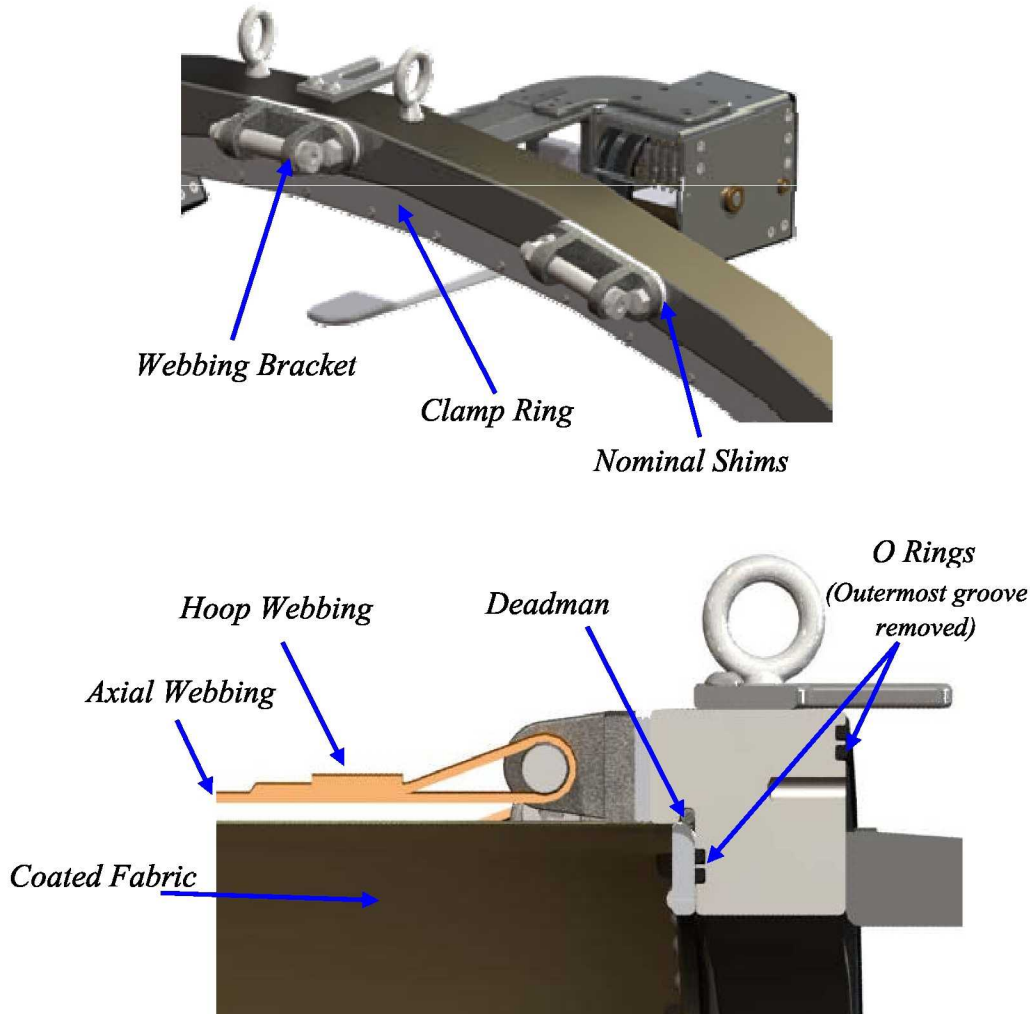
Figure 3.5. Interface ring softgoods side

Figure 3.6 illustrates the backside of the interface ring which is designed to integrate with the hard endcaps designed by LaRC using 72 x ½-13 threaded bolts. The 72 bolts were a design request by LaRC at the same radius of 59 inches as the axial webbing brackets. Three locating prongs were included for alignment with the hard endcaps. For packing purposes, packing plates, later packing rods, were designed to support the softgoods during the packing and deployment phases of operation.

Locating Prong

Lifting Eyebolts

Packing Plates

Endcap Bolt Holes

O Ring Grooves
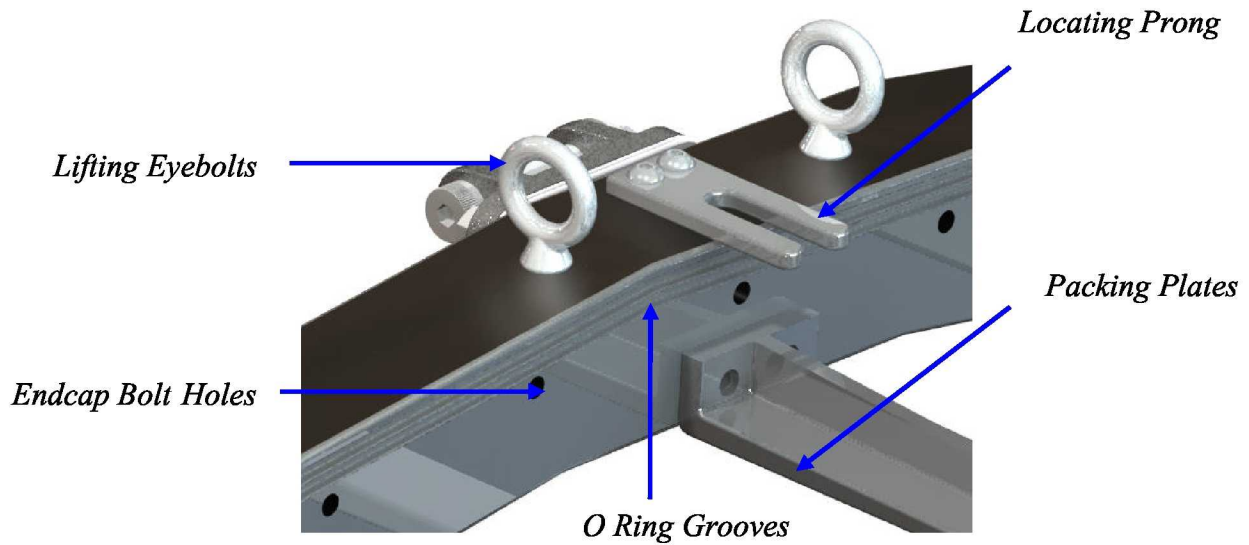
Figure 3.6. Interface ring endcap side

3.4   Window Design

The purpose of the window is to demonstrate the capability of a softgoods expandable structure to have a sealed cut-out included. While most conceptual lunar designs place a window on the hard structural components, X-Hab will prove the viability of packing and deploying a window in the expandable section.

The window design is detailed in Figure 3.7. The primary focus of this design is to allow the load path of the webbings to run around the window without terminating the webbings in the window frame.   The original concept for this window (Figure 3.8) used the same design techniques as the interface rings; terminating both the bladder and the webbings in the window frame and therefore requiring a much more substantial load handling capability from the window assembly.
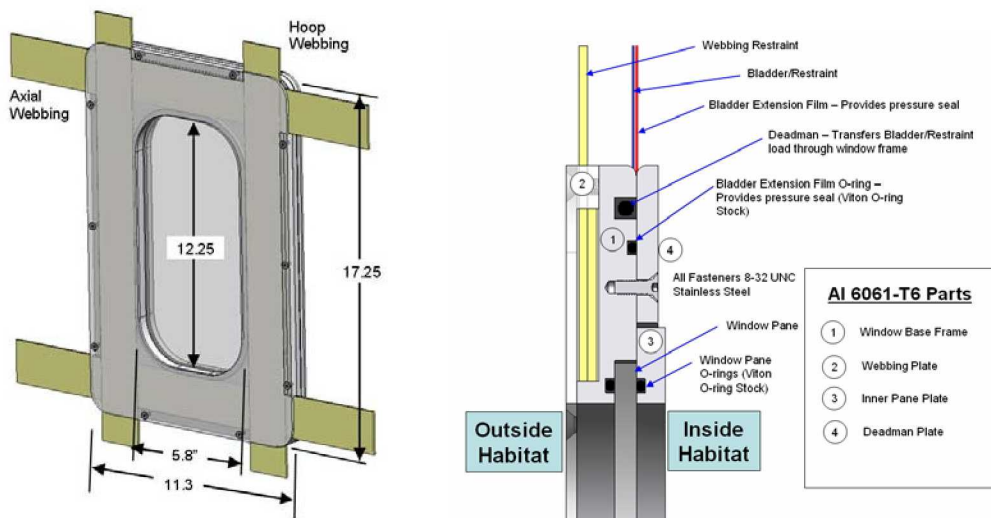
Figure 3.7. Final Demonstration window design
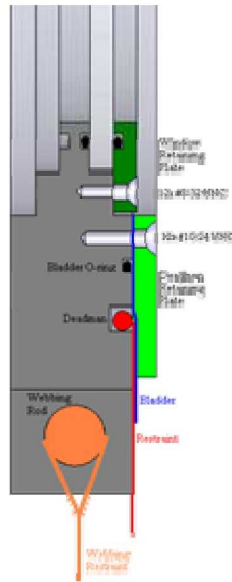
Figure 3.8. Initial Window Design

The final window design uses a double seal pane design with an o-ring on both faces of the window. The primary window frame (Window Base Frame) has an o-ring groove for one side of the window. The Inner Pane Plate mounts to the Window Base Frame and pinches the Window Pane in place. This design allows the pane to be removed from inside the X-hab without removing the assembly. The bladder/restraint layer termination uses the same technique as the Interface Ring. The Deadman and the o-ring are both held in place by the Deadman Plate. The webbings are routed over the top of the window using an encapsulating plate (Webbing Plate) to ensure proper position.

This design is for use in a prototype system, but is adapted from a design concept for an operational system. An operational system would include 4 window panes, which would accommodate a safe change out of any one pane. The one additional pane would stack on the inside of the habitat and two would stack on the outside. These would all be integrated using additional Window Pane Plates. Small channels and valves would be required to control the pressure between each window pane. Both the prototype and operational window were designed to meet the required hardware safety factor of two based on a 9 psi habitat.

3.5   Floor Design

The current floor fabricated for use in the Expandable Lunar Habitat is designed purely for demonstration on earth and has no application to a flight system (Figure 3.9). The flight version would be lightweight and deployable. The current robust, but heavy floor is designed to allow visitors to walk through the inside of the demonstration unit at low pressure.

The floor is made up of three aluminum I-beams that run parallel to the axis of the habitat. The beams are laid in place one at a time and can be carried by two people. Fiberglass grated panels are then placed and secured with fasteners into tapped holes on the I-beams. This approach allows quick and easy integration and disintegration of the floor and permits the floor to be transported with the habitat. The floor interface, at each end of the expandable section, is

14

versatile, allowing a deployable mechanical floor or inflatable floor system to be added in the future.
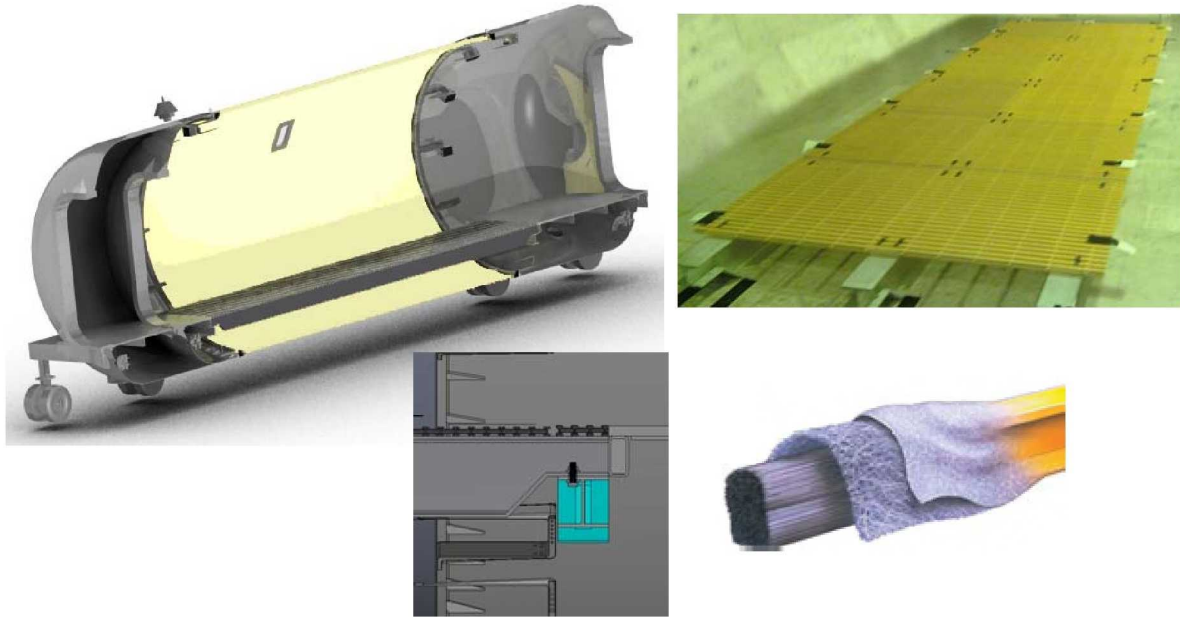
Figure 3.9. Floor images. *(Clockwise) Isometric model view. As built floor. Fibergrate floor core. Floor and endcap interface.*

3.6   Manufacturing Fixture

A manufacturing fixture is needed for the integration of the restraint layer and interface hardware. The manufacturing fixture is designed to support the weight of both interface rings and facilitate in the deployment and packaging trials conducted at ILC. A major goal of the packing and deployment trials was to determine the distance needed between the interface rings; therefore, the rings had to be able to pack as closely together as possible so as not to preclude any packaging scheme. Casters were attached to the fixture for deployment trials with the majority being swivel casters to allow easy positioning of the fixture and free motion in deployment. Figure 3.10 illustrates several views of this fixture.
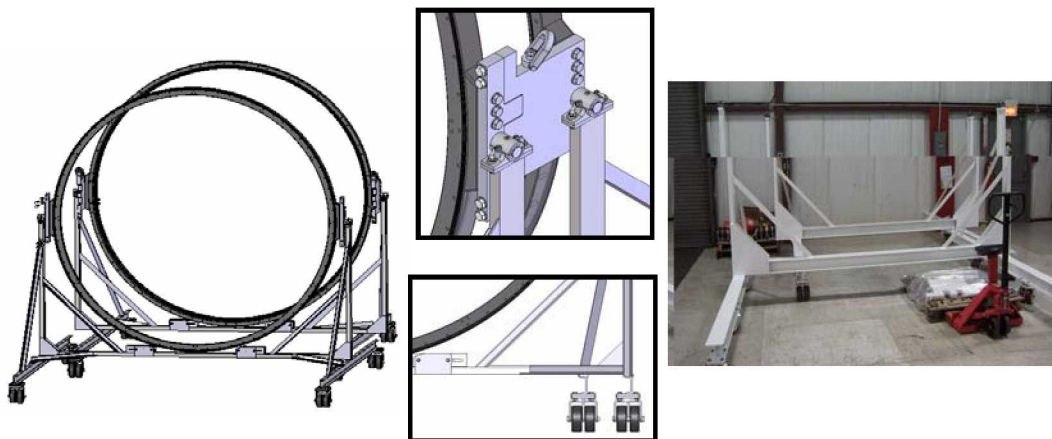
Figure 3.10. Manufacturing fixture.

To allow integration of the softgoods to the interface rings, the manufacturing fixture had to allow the rings to pivot. Split bearings were used to allow full rotation of the rings during integration which were then locked in place during deployment. A conceptual image of the softgoods integration process is shown in Figure 3.11.

Figure 3.11. Softgoods Installation

Analysis of the fixture was also conducted to ensure that the pin loading was within limits at the pivot point and that the gravitational loading on the ring during the horizontal position would not produce any additional stresses.

3.7 Packing and Deployment Hardware

The deployability and high packaging ratio of a softgoods expandable habitat is one of its primary benefits. Packing 'mandrels' are required on the back side of the interface rings to allow the softgoods to pack inside the endcaps. ILC has used this system in several programs. Mandrels are brackets or flat surfaces that are used to pack softgoods before deployment. The goal was also to provide a degree of control during deployment. This was hoped to be accomplished simply by the packing process but consideration was also given to a deployment mechanism. The initial packing and deployment hardware can be seen in Figure 3.12.
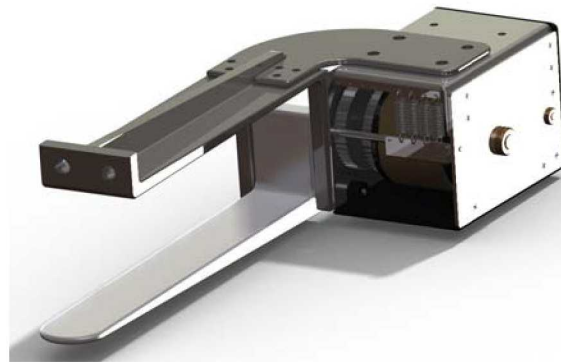
Figure 3.12. Initial Packing and Deployment Hardware

The deployment mechanism was designed to use a tensioned 2 inch wide strap to control the deployment. The mechanisms would be placed on the top half of the interface rings to slowly release material as the interface rings moved apart under inflation pressure. Figure 3.13 details the internal design and the analysis of the mechanism to determine the required tension.

16

$$\text{Tension} = \frac{40 \text{ lbf}}{2 * \sin(\theta)} = 77 \text{ lbf}$$

~120" θ ~15 deg.

θ

Windows

~ 40 lbf   ~82"   ~114"

Base of Ring

Height from the ring top to window top.

$$H_{window} := 114 \cdot in - 82 \cdot in \qquad H_{window} = 32 \cdot in$$

$$\theta_{cable} := atan\left(\frac{H_{window}}{120 \cdot in}\right)$$

$$\theta_{cable} = 14.931 \cdot deg$$

$$F_{tension} := \frac{\frac{wt_{lift}}{2}}{\sin(\theta_{cable})}$$

$$F_{tension} = 87.323 \cdot lbf$$
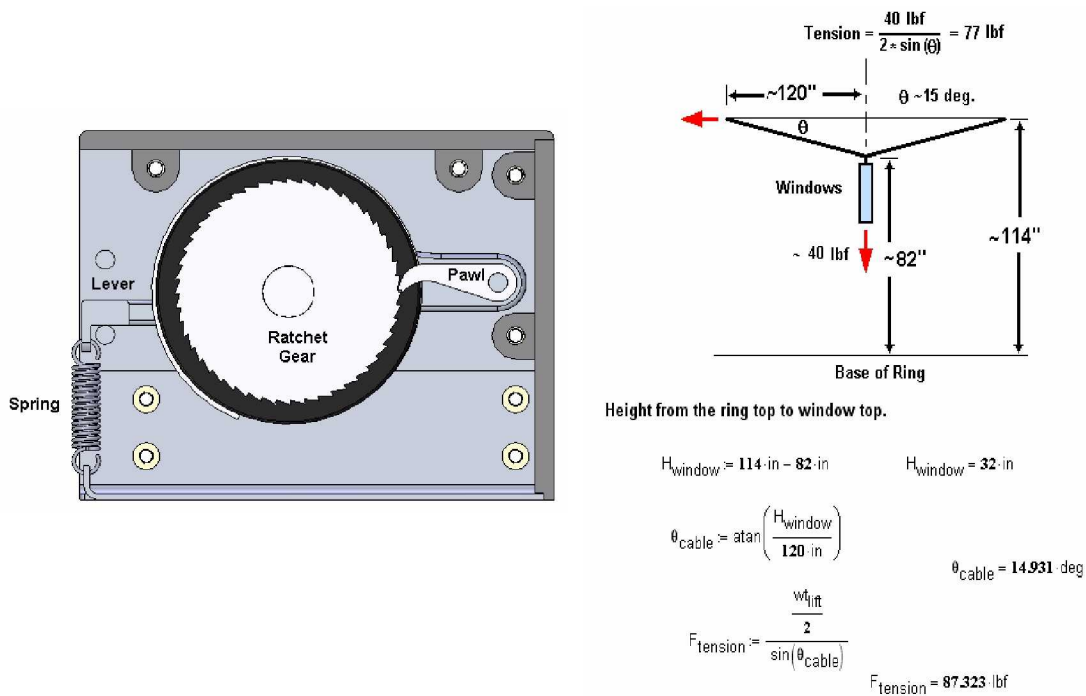
Figure 3.13. Deployment Mechanism

The deployment mechanism unfortunately had to be eliminated before manufacture due to program cost concerns. Also, with the addition of the TMC layer the hope was that in the future, controlled deployment could be accomplished with a mechanism attached to the outside or inside of the TMC. With the mechanism no longer attached to the packing bracket, the bracket could be greatly simplified to reduce costs. The packing bracket evolved in to a packing rod made of standard steel pipe parts. The packing rod was threaded into the back of the interface rings and used a compression fitting to allow easy installation and removal during packing. Figure 3.14 is an image of the packing rod and of the compression fitting.
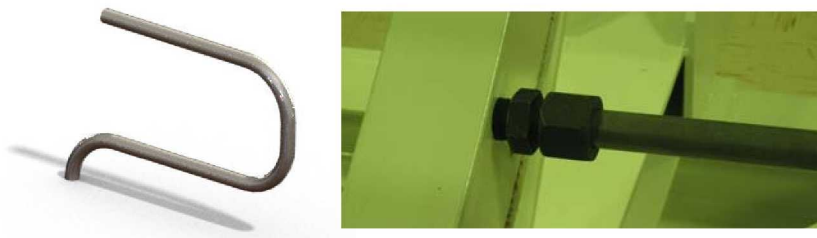
Figure 3.14. Packing Rod and Compression Fitting

4   Analysis

All of the analysis used the standard FEA package Abaqus® available from Simulia. The analysis was used to verify and complement the design process.

4.1   Fabric Lobe Analysis

A series of component-level finite element simulations were conducted to better understand the operational performance of the habitat's design[6]. The first of these was a study of the mechanical response of the bladder-restraint layer under an operational load of 9.0 psi. Using a component level approach, a single fabric lobe, or unit cell bounded by webbing was studied. Some of the fabric's relevant data are:

- Thickness: 0.0075"
- Yarn: 200 denier Vectran®
- Yarn count: 50 x 50
- Weave: Plain
- Coating: Urethane
- Ultimate Tensile Strength
    o Warp Direction: 551 lbs/in
    o Fill Direction: 520 lbs/in

A simple planar approach was used for the analysis, as the large radius of the cylindrical portion of the habitat causes the out-of-plane curvature of the unit cell to be negligible. The geometry consisted of a simple rectangle with the sides measuring from webbing edge to opposite webbing edge as shown in Figure 4.1. Using the webbing midpoints rather than the webbing edges builds some degree of conservatism into the analysis, as a larger unit cell would present more fabric stress. This modeling philosophy allows us to exclude the webbing from the simulation and still acquire a useful approximation of the fabric loading.
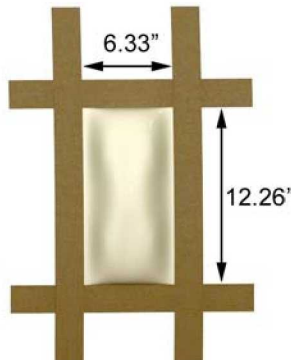
Figure 4.1. Geometry of the fabric unit cell studied under loading.

The step-wise sequence for applying the loads and boundary conditions in the model was quite straightforward. Nodes at all exterior edges of the unit cell's geometry had all translational and rotational degrees of freedom fixed. A pressure load of 9.0 psi was applied to one surface of the planar geometry and the material was subsequently oversized from the original shape by 1%. Over sizing was done analytically by assigning an appropriate thermal expansion coefficient to the material model along with an increase in a surrounding temperature field. The Abaqus finite

element software introduces this thermal over-sizing in a manner that does not pre-load the material and influence the final stress results. Analytical thermal behavior was carried out using the well known relationship given in Equation 2.

$$\Delta L/L = \alpha \Delta T \qquad (2)$$

The thermally induced strain is the product of the temperature change, ΔT, and thermal expansion coefficient α. In this case a strain of 0.01 was desired. A 100 degree temperature applied, leaving α to be 0.0001.

The material to be used in the analysis was first tested for its mechanical performance via uniaxial tensile tests in both the warp and fill directions. Data from these tests shows that the stress-strain response of the Vectran® fabric is both nonlinear and orthotropic. The fill direction has significantly lower modulus at low strain values compared to the warp direction as seen in Figure 4.2. This phenomenon was observed when the load on a given sample was cycled in the tensile frame. The tensile results were consistent from test to test, with a total of five tests conducted in the warp and fill. The stress-strain plot for one of these tests is shown in Figure 4.2.
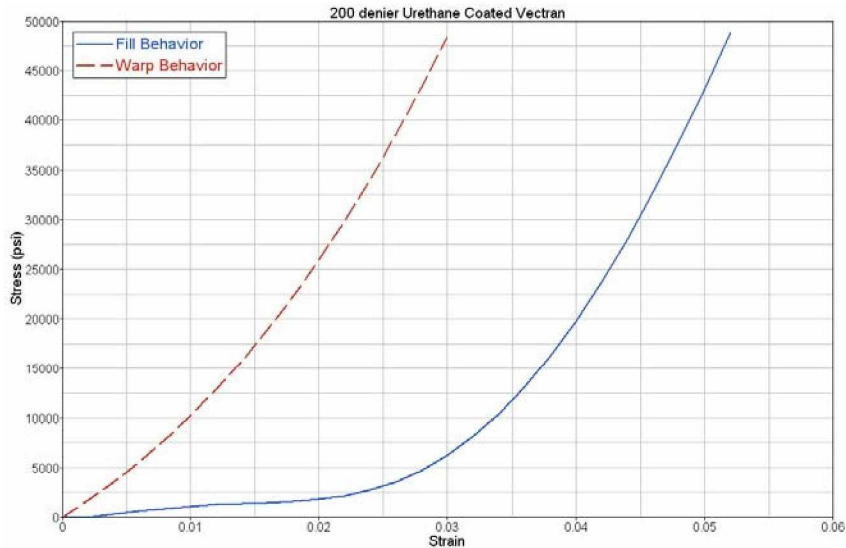
Figure 4.2. Stress-strain behavior for warp/fill directions of the 200 denier urethane-coated Vectran used in the analyses.

The corresponding plots of principal stress vectors indicate that the fill direction tends to drive the general pressure-induced radius of curvature in the unit cell, and contributes most to the fabric's elastic behavior under loading. The fill direction corresponds to a much lower modulus for low strain values, and is aligned with the short direction of the unit cell, running parallel with the 8.33" dimension. This behavior can be seen in Figure 4.3.
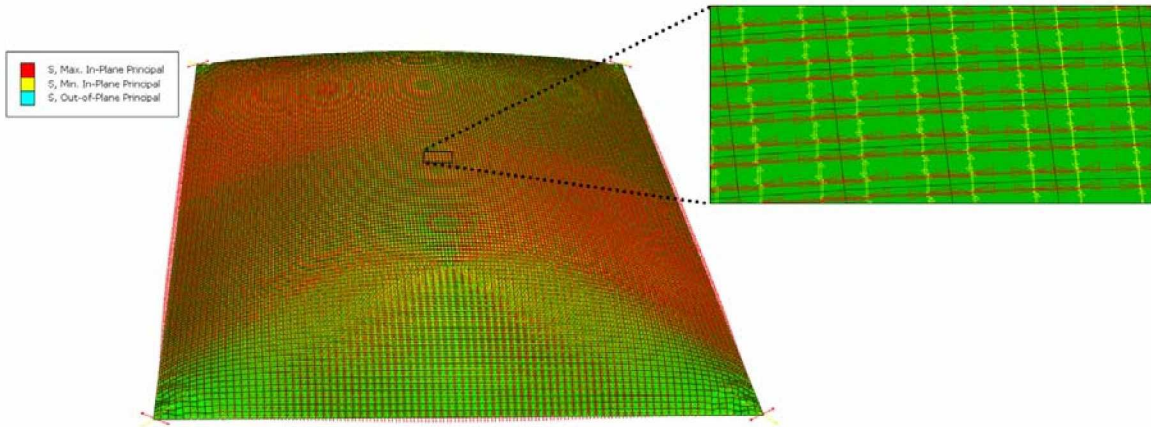
Figure 4.3. Principal stress directions for the fabric unit cell under a 9.0 psi pressure load. The red arrows indicate the maximum principal stress direction.

The final shape and stress contours for the isotropic, fill direction simulation are shown below. For the isotropic fill direction behavior, stresses near the center correspond to 74 lbs/in and stresses near the longer side equate to 84 lbs/in., as seen in Figure 4.4. Since the ultimate tensile strengths of the material in the warp and fill directions are 551 lbs/in and 520 lbs/in, respectively, the result is a higher safety factor than required.
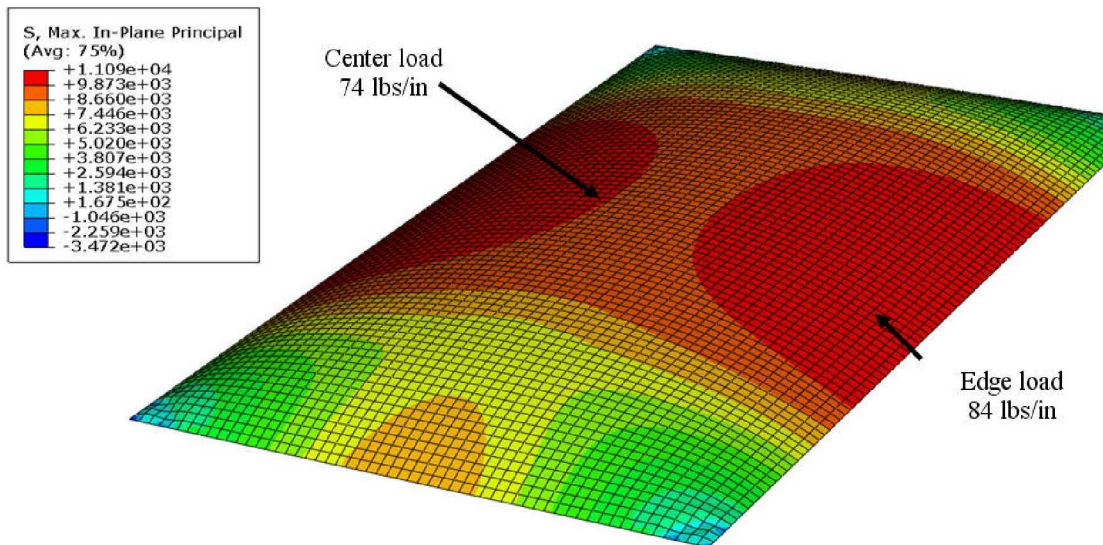
Figure 4.4. Material lobe loading

4.2   Webbing Analysis

In addition to the local loading of the bladder-restraint layer, another critical design consideration is the uniform loading of the interface rings. The uniform loading stems from the

axial webbings being cut and sewn to a specific length tolerance. To identify this tolerance, a finite element study was carried out on a component-level, simplified geometry of the habitat. All 26 axial webbings were included in the simulation; with one end of the webbings contacting a rigid, circular plate and the other end held fixed, as shown in Figure 4.5. A plug load of 9.0 psi was applied to the surface of the circular plate, simulating the axial effects of the habitat's nominal inflation pressure. Boundary conditions were applied which restricted the plate to only move in the axial direction. Results of interest include the elongation of the webbing, as well as the corresponding maximum in-plane stress
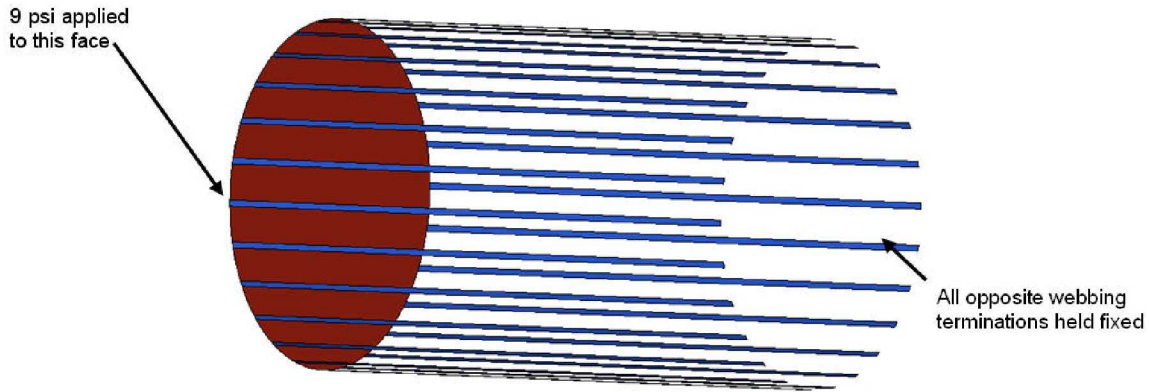
Figure 4.5 Webbing analysis setup

Figure 4.6 shows a contour plot of the elongation of the webbings when the habitat is inflated to a nominal pressure of 9.0 psi. The total axial elongation of the webbings for this case is 1.4".
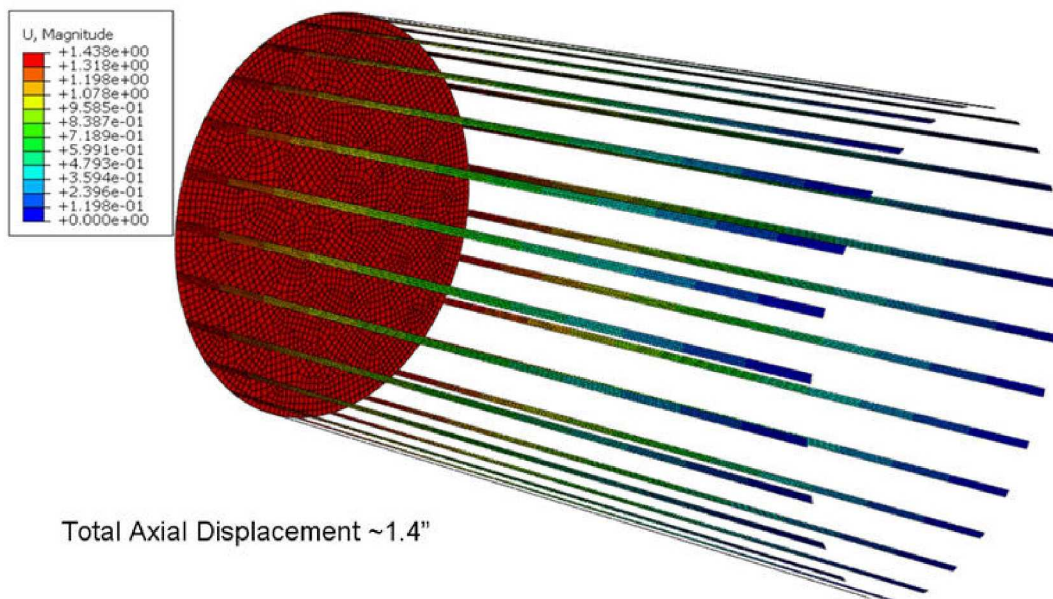
Figure 4.6. Webbing contour plot

A useful aspect of this model is the ability to adjust the length of the axial webbings to simulate manufacturing uncertainties. The worst scenario of inadvertent webbing shortening from a stress standpoint is the case where only one of the 26 axial webbings is foreshortened. Figure 4.7 shows a stress contour plot for the scenario where one axial webbing is ¼" or 0.125% shorter than the others, again done analytically via thermal contraction, as described above. As with other fabric materials in the habitat's analysis, membrane elements were used for the webbing material, which accounts for the material's low bending resistance.
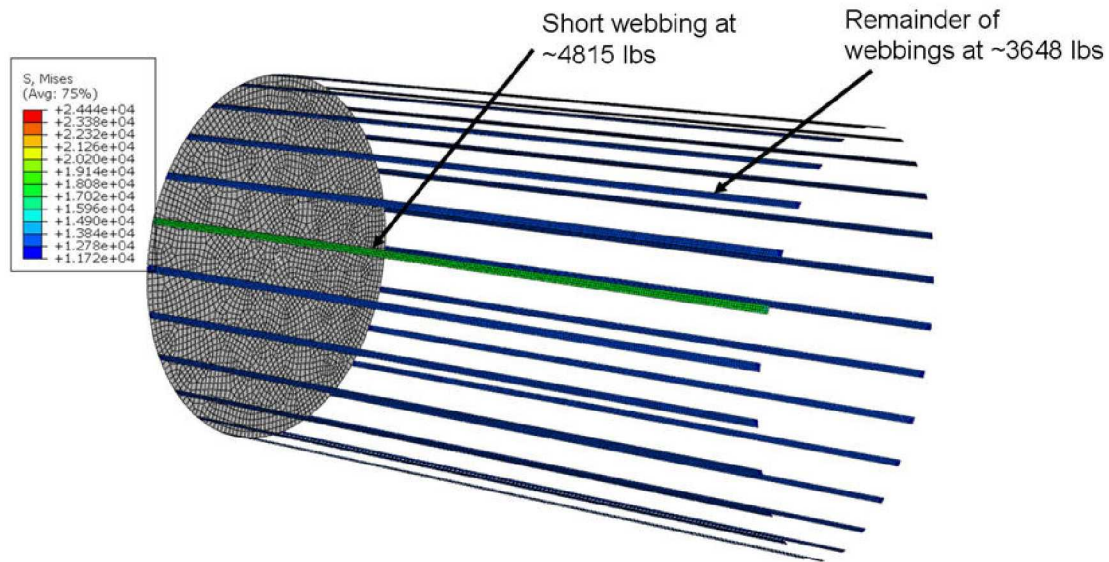
Figure 4.7. Webbing tolerance analysis

In this case, the Mises stress in the shortened webbing corresponds to a force of 4815 lbs, while the remainder of the webbings experience a force of 3648 lbs. The advertised breaking strength of the axial webbing is 24,000 lbs, so the result is a higher safety factor than the required four.

4.3   Hardware Analysis

FEA was performed on the critical, custom hardware components to ensure that the desired safety factor of 2 was satisfied in all cases.

4.3.1   Interface Ring

In order to understand the mechanical performance of the attachment ring that interfaces the hardware to the softgoods, a simple FEA analysis was conducted. Since the ring was designed with two-fold rotational symmetry, a quarter of the geometry was used for the analysis. Figure 4.8 shows a circular pattern of the geometry used which represents the entire ring. Appropriate symmetry boundary conditions were applied to the nodes at the termination of the quarter geometry.

22

Figure 4.8. Attachment ring shown as an entire part. To simplify the analysis, only a quarter of the geometry was used for the finite element analysis.

A36 steel was used as the material in the analysis, with the assumption that the stress-strain behavior is linearly elastic and isotropic. The yield strength of the material was taken to be 36,000 lbs/in^2.

The nodes corresponding to the bolt holes that attach to the habitat's end caps were held fixed, with no rotational or translational degrees of freedom. To simulate the inflation load, 24,605 lbs was applied to the bolt holes on the bracket/fabric side. The results are shown in Figure 4.9 as a contour plot of Mises stress.
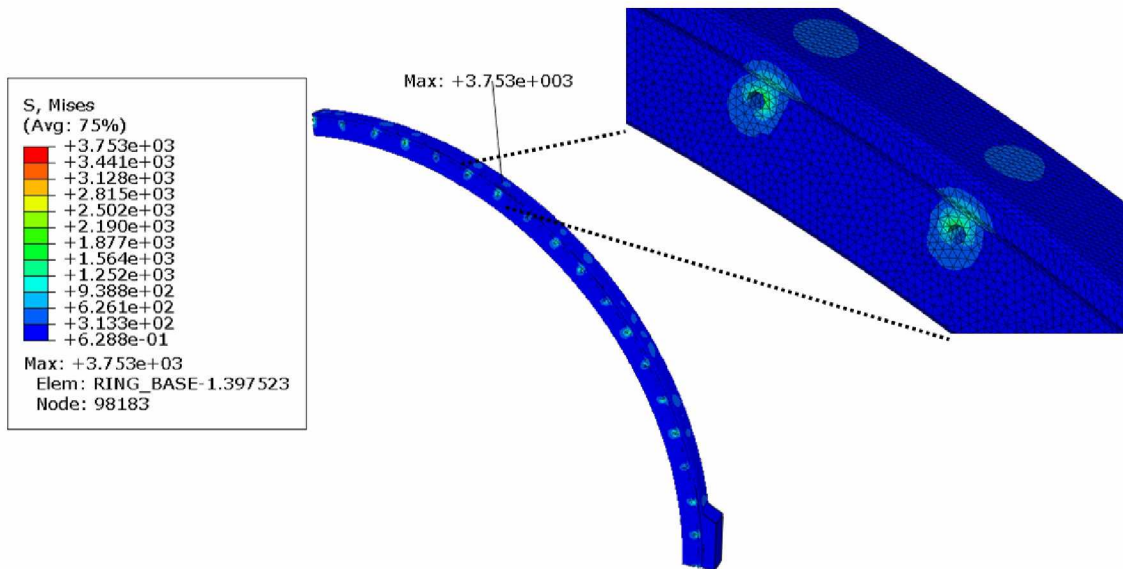
Figure 4.9. Contour plot of Mises stress for the hardware attachment ring.

Some regions of the geometry show small pockets of higher stresses, on the order of 3750 lbs/in^2, although these values are likely due to localized areas of misshapen elements, and are inherent to the mesh itself. A more reasonable quantity of ~3400 lbs/in^2 is taken to be the high stress value; this corresponds to a factor of safety of ~7.4.

4.3.2 Bracket

The bracket was analyzed to determine the proper configuration and clevis pin for the expected loading. The bracket was designed to a safety factor of 2 over the expected loading conditions. Using the FEA analysis package, 'Simulation' (formally COSMOS) a pin size of .71 inches in diameter was determined as necessary. For cost reduction purposes, a standard shoulder bolt with .75 inch diameter was used in the final design. Since the webbing is free to rotate at several angles, the bracket would be partially loaded in several configurations. The hoop webbing also impacts the angle of loading on the bracket. Conservatism was built into the design by fully loading the bracket to the worse possible off angle. Using this approach, the initial bracket design was optimized for the lowest mass while maintaining a safety factor of 2. Figure 4.10 is a picture of the bracket detailing the highest stress locations in red.
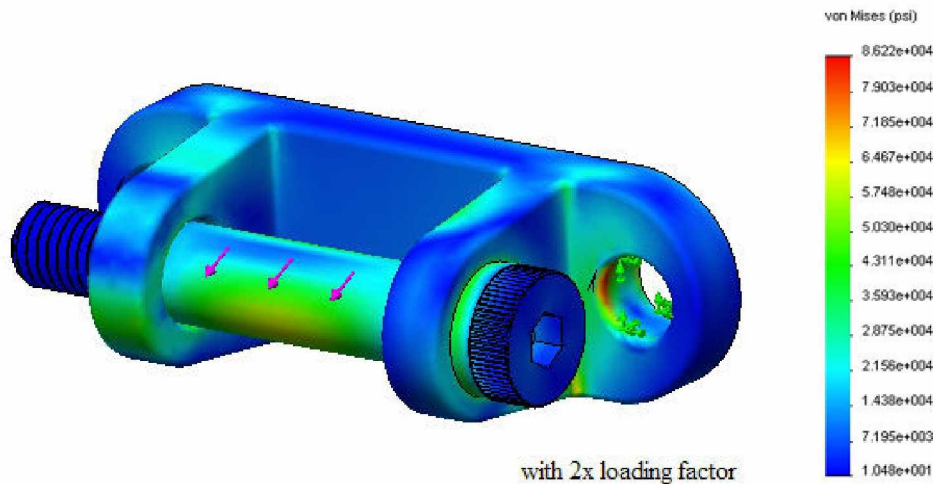
Figure 4.10. Bracket Analysis

4.3.3 Window

In addition to the hardware interface ring, an FEA study was carried out to understand the mechanical properties of the habitat's window under a nominal inflation pressure of 9.0 psi.   The geometry corresponding to the airplane style window was used for the analysis. The metal frame was assumed to be constructed of 6061-T6 aluminum which has a yield strength of 42,000 lbs/in^2, and the window was taken to be constructed of a bullet-resistant polycarbonate material, having a yield strength of 8250 lbs/in^2. The elastic modulus of the polycarbonate was taken to be 312,000 lbs/in^2.

Separate components that are in contact with each other in the design, either by bolting or compression, were assigned an analytical surface-to-surface contact boundary condition and were held together using Abaqus's TIE constraint. The fully assembled geometry used in the analysis and corresponding finite element mesh is shown below in Figure 4.11.

Figure 4.11. Fully assembled geometry and finite element mesh used in the habitat's window analysis.

In order to react the internal pressure load analytically, the edges of the interior frame were assigned a "pinned" boundary condition. That is, while nodal rotational degrees of freedom were permitted, translational motion was prohibited. The edges that were pinned on the frame are shown below in Figure 4.12.
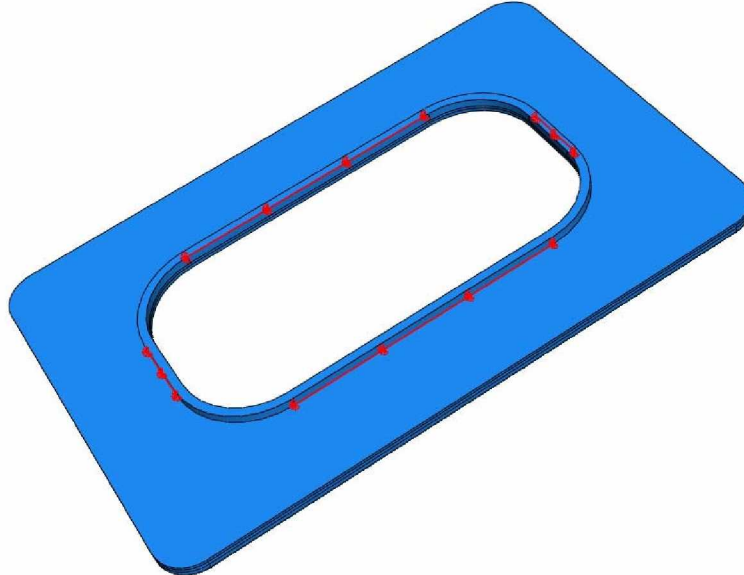
Figure 4.12. Interior frame for the window analysis. Edges that were assigned to have no translational degrees of freedom are shown in red.

To simulate loading due to inflation, a pressure load of 9.0 psi was applied to the entire interior surface of the window assembly. Figure 4.13 below shows a contour plot of Mises stress under a 9.0 psi pressure load. A peak Mises stress of 9,215 lbs/in^2 is reported, although this value is likely due to local discontinuities in the mesh. A more representative value that reflects the

actual maximum Mises stress is ~5400 lbs/in^2; this represents a factor of safety of ~7.8 with respect to the yielding of Al 6061-T6.
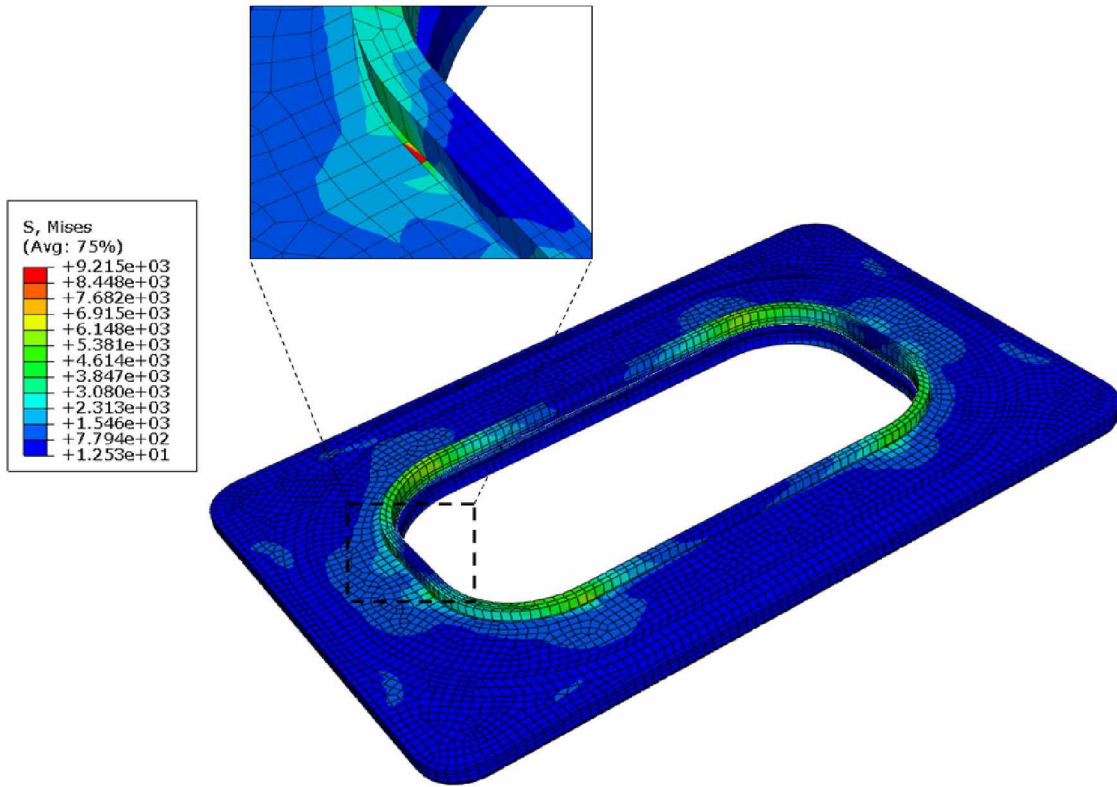
Figure 4.13. Contour plot of Mises stress for the hardware component of the window under a 9.0 psi pressure load. *The breakout box shows a region of a mesh-based stress concentration. Actual maximum Mises stress is ~5400 lbs/in^2.*

Figure 4.14 provides a similar view of the polycarbonate window component, where Mises stress is shown from a 9.0 psi pressure load. A maximum value of 2,167 lbs/in^2 is given, which represents a safety factor of ~3.8.
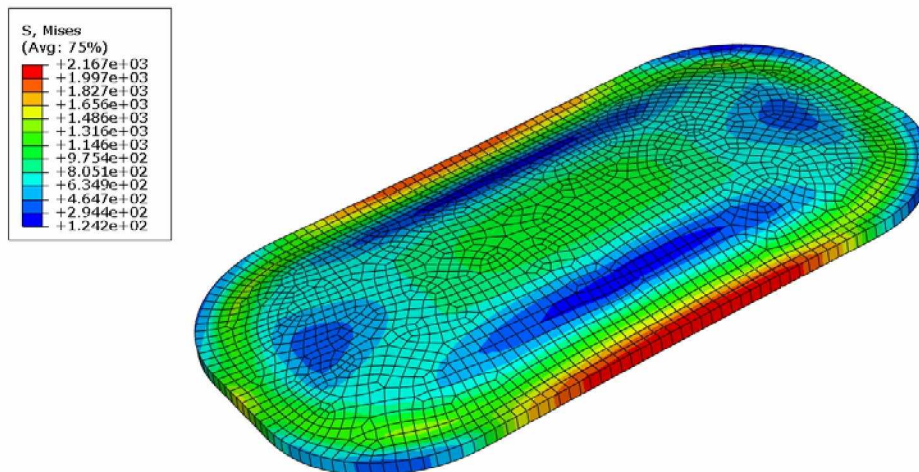
Figure 4.14. Contour plot of Mises stress for the polycarbonate component of the window.

26

5 Testing

All textile materials included in the habitat are submitted for performance verification tests. These evaluations ensure that the component materials are capable of sustaining the intended stresses and loads. Upon their acceptance for use, design subassemblies are tested to verify their performance capability before final integration into the article. The overall test program includes but is not limited to the performance tests found in Table 5.1.

Table 5.1 Overall Test Program of Softgoods and Design Components

Performance Characteristic	Test Method
Basecloth	
Weight	ASTM D 3776 (Fed-Std-191, TM 5400)
Tensile Strength	ASTM D 5035 (Fed-Std-191, TM 5102)
Finished Fabric	
Weight	ASTM D 3776 (Fed-Std-191, TM 5400)
Tensile Strength	ASTM D 5035 (Fed-Std-191, TM 5102)
Tear Strength	MIL-C-21189, TM 10.2.4
Peel Adhesion	ASTM D 751 (Fed-Std-191, TM 5970)
Seam Constructions	ASTM D 5034
Air Permeability	ILC Test Method
Flame Resistance, Vertical	ASTM D 6413-99 (Fed-Std-191, TM 5903)
Webbings	
Width/Thickness	ASTM D 3774/ASTM D 1777
Weight	ASTM D 3776
Tensile Strength	ASTM D 5035
Seamed Strength	ASTM D 5035
Sub-Assemblies	
Fabric Interface with End-Caps	ILC Test Method
Fabric Lobe Evaluations	ILC Test Method
Webbing Take-Up Assessment	ILC Test Method
Webbing Termination to Hardware	ILC Test Method

5.1 Fabric Testing

Structural analysis determined the minimum tensile capacity required for the habitat and drove the selection of all materials. The minimum tensile requirement for the bladder fabric was 400 lbs/inch and therefore, various materials were researched that would accommodate this requirement. The selected material was excess fabric from the MER Impact Landing Airbag program that NASA graciously made available for use on the habitat program.

During a requirements review prior to the fabrication of the habitat, the question was raised whether or not a Flammability Requirement (FR) should be imposed on the softgoods. Though previously not specified, it was determined that a flammability requirement should be imposed on the bladder fabric. Numerous building codes and standardized flammability test methods were reviewed for applicability to this prototype habitat application. The study report, *Evaluation of Flammability Standards and Test Methodologies for Applicability to the Expandable Lunar Module Test Unit* was generated and submitted to the NASA LaRC team for review on July 16, 2008. It presents the results of the flammability investigation and includes the flammability performance of a similarly constructed Vectran fabric (as intended for the gas retaining bladder) that was treated to meet a 15 second burn and 8 inch char length when tested, in accordance with Federal Standard 191A, Test Method 5903. Following that review, it was agreed that the FR bladder fabric would be constructed to meet at a maximum, the 15 second burn and 8 inch char length performance when tested against Federal Standard 191A, Test Method 5903.

As stated earlier, the amount of coating applied to a fabric for FR capability and gas retention can significantly change its performance properties. The properties that have the most impact on the habitat performance are flexibility and weight. As more coating material is added, the flexibility of the fabric decreases. This could have a significant impact on the prototype performance. Therefore, ILC strove to minimize the effect that the additional FR processing conditions imposed on the basecloth while optimizing flexibility performance.

Table 5.2 lists all specified characteristics, requirements, test standards, and resultant acceptance test data of the finished coated/laminated bladder fabric.

Table 5.2 Physical Properties of the Bladder Fabric

Performance Characteristic	Test Method	Requirement	Mean Acceptance Performance Values
Weight (oz/yd^2)	ASTM D 3776 (Fed-Std-191, TM 5400)	7.0 $\pm$ 0.2	7.00
Tensile Break Strength (lbs/inch) warp x fill	ASTM D 5035 (Fed-Std-191, TM 5102)	400.0 minimum	525 x 523
Tear Strength (lbs) warp x fill	Mil-C-21189, TM 10.2.4	50 x 40	63 x 56
Peel Adhesion (lbs)	ASTM D 751 (Fed-Std-191, TM 5970)	8.0 minimum	13.0
Air Permeability @ 9.0 psi (scc/min/cm^2)	ILC Test Method	Zero Leakage when tested at 9.0 psi	Pass
Flame Resistance, Vertical	ASTM D 6413-99 (Fed-Std-191, TM 5903)	Burn Time $\leq$ 15.0 seconds Char Length $\leq$ 8.0 inches	warp burn time 2.5' char length - 2.75" fill burn time 2.22' char length 3.0"

The properties of the basecloth were pre-determined due to the use of an available material. However, due to the coating / lamination processes it was anticipated that the flexibility, weight, permeability and FR performance properties could all be impacted.

The desired FR performance drove the selection and composition of the materials used for this processing application, and that application was driven by the performance requirements specified in the fabrication of the final goods. The material remains very flexible so as not to impact packing and deployment procedures and did not leak when pressurized with air in ambient conditions at 9.0 psi.

For a reduced mass system, the goal was to have heat sealed seams for the gas retention layer. Seam selection was based on previous softgoods work at ILC. Specifically the webbing net design of the CEV Generation II airbag system provided the initial seam characteristics. After several seam evaluations a final configuration was decided on. This configuration used a single 2 inch wide structural tape with no cover tape which exceeded the minimum 400 lbs/in. A cover tape is a tape applied to the outside of the fabric that is used to assist with flexing and load reduction. However, since a habitat does not see high flexing, and this design has webbings over all of the seams, a cover tape was deemed unnecessary.

5.2   Webbing Testing

Two inch wide Vectran webbing was chosen for the webbing net of the habitat. The webbing net consisted of both axial and hoop webbings. The axial webbings terminated in sewn loops on each end that were attached to pin clevis brackets on the interface rings. Hoop webbings were sewn, continuous loops that traveled around the circumference of the habitat. The hoop webbings were undersized by 1% to induce loading of the webbing net before the fabric. The axial webbings were line-on-line. This refers to the fact that the axial webbings were patterned to follow the hoop webbings and were not subsequently oversized in length since the analysis demonstrated the elongation properties of the webbing.

Two different strengths of webbing were initially considered for the habitat; a 12,000lb webbing and a 24,000lb webbing. These were first to be used in combination, with the 12k used for the axial webbings and the 24k used for the hoop webbings. In this design, there were 33 of each type of webbing. However, as the analysis of the design progressed, the decision was made to instead use only 24k webbing. This resulted in the use of 26 axial webbings and 24 hoop webbings that still met the required safety factor of 4.

The following section covers the testing performed on the webbing stitch patterns, both for the initial design and for the final design. Table 5.3 is a summary of the acceptance testing on the webbing.

Table 5.3 Physical Properties of the 24k Webbing

Performance Characteristic	Test Method	Requirement	Mean Acceptance Performance Values
Width (inches)	ASTM D 3774	2.0	2.03
Thickness (inches)	ASTM D 1777	0.12	0.122
Weight (oz/yd^2)	ASTM D 3776	3.2	3.19
Minimum Tensile Break Strength (lbs)	ASTM D 5035	24,000	28,780

5.2.1 *Webbing Take-Up Assessment*

Stitching take-up is seen in sewn products due to the tension imparted to the thread by the machine while stitching the seam. This causes the base fabric, or in this case webbing, in which the seam is sewn to shorten slightly. The amount of take-up varies based on the type of stitching, type of thread, machine settings, and length of stitching. To quantify and account for this loss, testing was performed on the stitch patterns selected for the webbing loops. This was critical in order to meet the webbing length tolerance found during the analysis of the loading on the endcap rings.
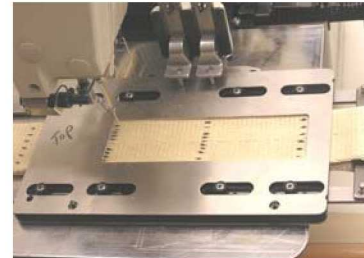
Figure 5.1 Webbing Stitching

Table 5.4 gives a summary of the test results for the webbing take up. Figure 5.1 shows the fabrication of the webbing. Over a 12 inch stitch pattern about a ¼ inch reduction was seen in the webbing length. Although the critical aspect of this design was making all of the webbings the same length, it was also important that the final length of all the webbings be in a desired range as well. The testing procedure resulted in a testing error of .0625 inches.

Table 5.4 Summary of Webbing Take-Up

Test #	Test sample	Test description	Seam description	Total number of samples tested	Average Take-Up (in)
1	12k	12 inch sample, length measured before and after sewing	Diamond(opposing "V" Stitch) (length – 6 inch)	5	0.125
2	24k	12 inch sample, length measured before and after sewing	Diamond(opposing "V" Stitch)(length -6 inch)	5	0.125
3	12k	12 inch sample, length measured before and after sewing	Eye to eye (9 in seam)	5	0.5
4	12k	60 inch sample, length measured before and after sewing	Endless loop (12 in seam)	5	0.25
5	24k	12 inch sample, length measured before and after sewing	Eye to eye (9 in seam)	5	0.125
6	24k	36 inch sample, length measured before and after sewing	Endless loop (12 in seam)	5	0.25
7	24k	12 inch sample, length measured before and after sewing(UR 108" applied to the webbing before sewing)	Eye to eye (9 in seam)	5	0.25
8	24k	60 inch sample, length measured before and after sewing(UR 108" applied to the webbing before sewing)	Endless loop (12 in seam)	5	0.25

5.2.2 Webbing Seam Configuration

The first type of seam selected was an overlapped diamond stitch pattern. Two six inch diamond stitch patterns were sewn using an automatic sewing machine. The advantages to the automatic sewing machine were to reduce variability in stitching, therefore having a more consistent length between webbings. The drawback to this method was the travel of the machine prevented the length of the stitch pattern from exceeding six inches. This resulted in the use of two six inch patterns, overlapping for three inches at the center, with a total length of nine inches. This seam was used for both the axial and hoop webbings.

Both the 12k and 24k webbing were tested. For each test, the webbing was marked, measured, and clamped in the fixturing of the automatic sewing machine. Once the stitching was complete, the webbing was measured again. The 12k webbing was seen to have a consistent take-up of 1/8 inch for a nine inch seam. The take-up in the 24k webbing ranged from zero take-up to a maximum take-up of ¼ inch for a 9 inch seam. This is likely due to the difference in flexibility of the 24k webbing, when compared to the 12k webbing.

To meet the 4x factor of safety, all seams needed to meet a tensile strength of 18,000lbs. Axial seam samples were fabricated and tested at ILC Dover to 20,000lbs with no signs of failure; however, given the capability of the test equipment, the samples could not be taken all the way to failure. In order to test the hoop webbing configuration, sewn as a continuous loop, the samples needed to be tested to 36,000 lbs. This is due to the load sharing of the webbing as it is set up for the test, with the loop being held with pins at the top and bottom of the loop. This means that load is being shared equally between the side of the loop with the seam and on the non-sewn side. This testing was performed at Stork Climax Research Services. The results showed that while the samples averaged 36,660lb, with a load on the seam of 18,330lb, there were several individual samples which fell short of the requirement at roughly 16,000lb. The data for the stitch samples can be seen in Appendix D. Due to these failures, several new seam stitch patterns were evaluated for use. These included different stitching layouts as well as thread types. A single 12" long diamond stitch pattern was selected. This was sewn by an experienced operator using a marking template. This was tested only in the 24k webbing, since the overall webbing net design had been finalized at this point.

Tensile tests of the sewn 24k webbing loops were also performed at Stork Climax Research, using the same test setup as used previously. The average tensile strength of the samples was 38,740lb, with a minimum breaking strength for a single seam sample of 18,690lb.

Webbing stretch under load was also accounted for by preloading the webbings prior to manufacturing. All webbings were inspected before being integrated into the webbing net and proofed to 1.5x the load they would have to sustain with the EDU at full pressure (9 psi).

5.2.3 Creep Testing

ILC and LaRC developed a test regimen to characterize the effect of sustained loading of the Vectran webbings used in the construction of the restraint layer of the habitat. The ultimate objective of these tests is to make predictions on the time to failure based on the stress conditions that the webbings will be subjected to. This analysis is critical to ensuring the continued performance of the restraint layer throughout the intended life cycle of the lunar habitat. The creep test methodology was developed based on creep testing high performance materials for Inflatable structures and the creep characterization of textile composites. Since manifesting a creep failure in a specimen under real-time loading conditions is unrealistic due to the long time

frame involved, the process of creep failure is predicted by employing the Time Temperature Superposition (TTS) principle. The creep failure of Vectran webbing, using this test method, can be achieved in a relatively short period of time (approximately one day) by subjecting the Vectran specimen to periodic increases in temperature under a constant load of approximately 50~70% of the Ultimate Tensile Strength (UTS).

The Vectran webbings used in this application have a high UTS, thus they require a high load capacity tensile test machine. In addition, an environmental chamber is needed that can accurately achieve and maintain the temperature steps required to complete a creep test. The creep testing includes four categories of webbing samples, namely: pristine, folded, sewn seam and thermally aged. The folded samples simulate the webbing sections that would be folded due to packing of the habitat.

The testing is currently being conducted at LaRC. Seam and creep testing will be used to further understand the structural behavior of the EDU and assist with future design iterations.

5.3   Subassembly Testing

Subscale testing along with manufacturing acceptance procedures of several components was completed as a risk mitigation procedure.

5.3.1   Fabric Lobe Fixture

A critical aspect of the X-hab design is the lobing of the fabric between the webbings. The lobe is a geometric nonlinear structure where the magnitude of the deformations influences the resultant stress state. As the magnitude of the local pillowing deformation in the lobe increases, the maximum tensile stresses in the lobe fabric fall. This results from the lower overall radius of the arcs running across the lobe from webbing to webbing. Having a good prediction and overall understanding of this lobe deformation would allow for a better system mass optimization. As a result, a load test was designed for the lobe as a risk mitigation.

Since there was neither time nor budget to develop a new fixture for the habitat lobe, an existing fixture was implemented. This fixture was developed and fabricated under a different program with moderately different experimental objectives and is shown in Figure 5.2. In this program the experimental objectives regarding deformation were more qualitative then quantitative. Despite these differences it was decided to give this existing fixture a try and also determine its suitability for any future X-hab work.
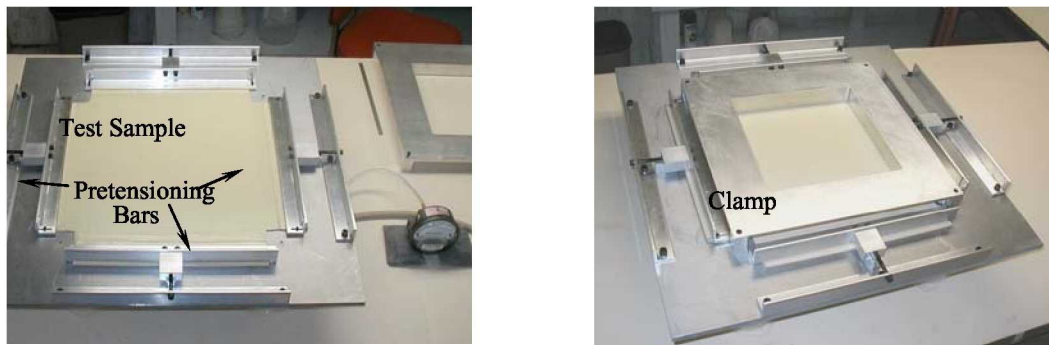

Figure 5.2. Fabric lobe test fixture

The test article was a cruciform shaped piece of the lobe fabric with a deadman system to preload the fabric in the testing fixture. A rectangular grid was marked on the cut test article for the placement of the photogrammetry targets. The 'frame' clamped down on a rubber gasket to permit inflation gas retention under the test article. Figure 5.3 is a top view of the test setup. Inflation pressure was applied to the backside of the fabric and the 'frame' clamped down on to the rubber gasket. The pressure was taken up in 1 psi increments until the point where the internal pressure overcame the sealing capacity of the gasket and the available shop air. Photos were taken at each inflation point as required for the photogrammetry calculations.
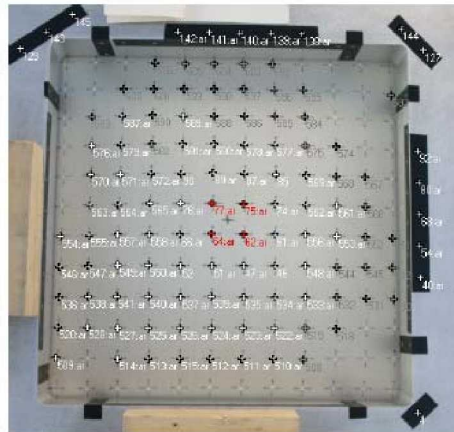
Figure 5.3. Fabric lobe test setup

During actual testing the maximum attainable inflation pressure ended up between 5.0 and 6.0 psi. At this point, the leakage through the gasket was so great that the available shop air could not provide any additional pressure differential. As a result we choose the 5.0 psi measurement for our first detailed look at the data. Some problems with the lighting conditions resulted in a smaller field of targets that could be auto marked in the Photogrammetry post-processing.
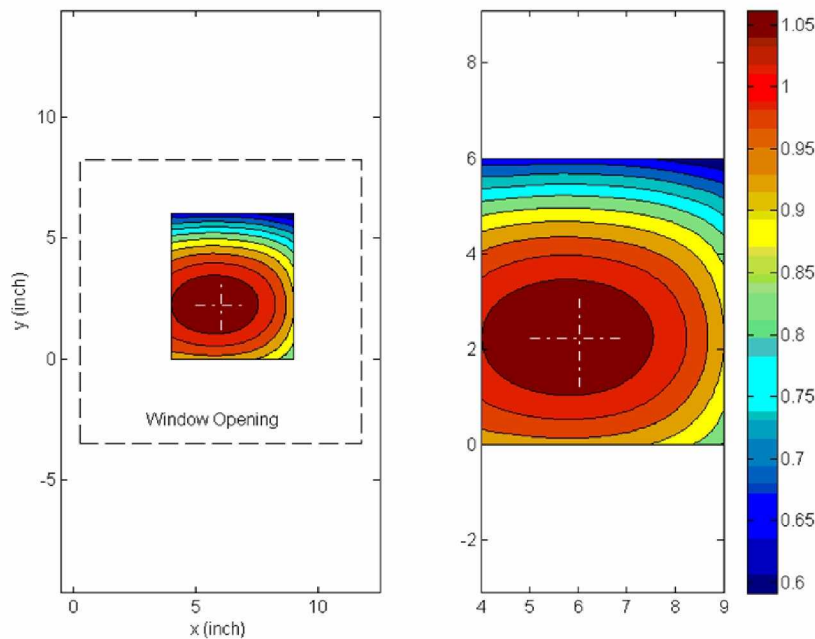
Figure 5.4. Contour plot

Figure 5.4 shows where the frame clamp was (dashed line) and where targets could be marked and resolved (contour plot). This contour plot shows the vertical displacement of the lobe fabric (in). Figure 5.5 shows a 3D view of the same displacement contour plot.
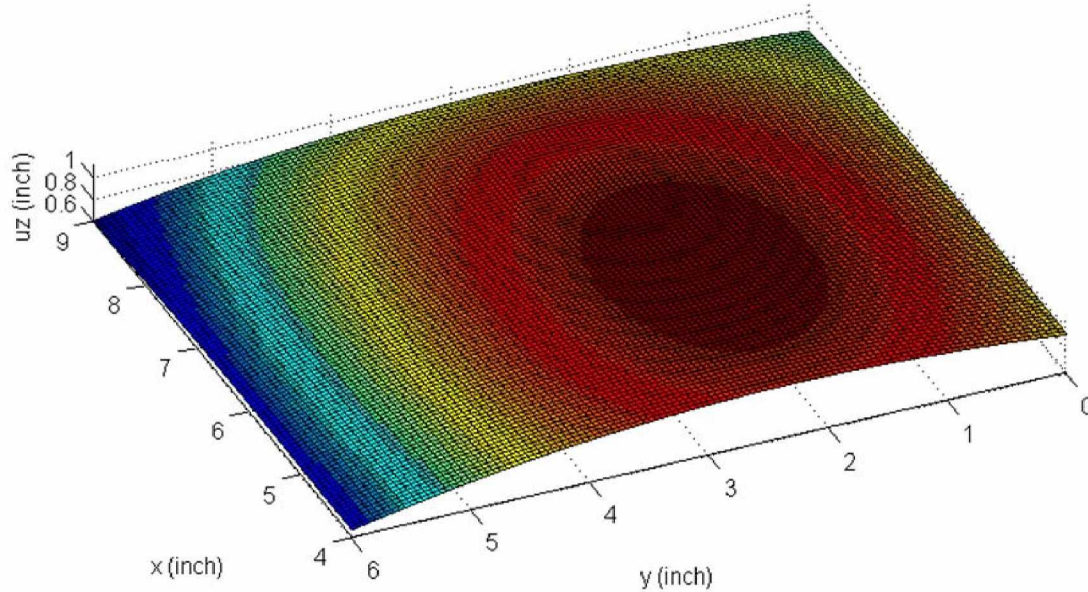
Figure 5.5. 3D Contour Plot

Analysis results from an FE model corresponding to the geometry of the test setup was compared to the results of the experiment. Some significant differences were immediately noted for the measure of maximum vertical displacement. A detailed examination of the test data determined that a significant amount of material had slipped through the clamp region during the test. The FEM window edges were fixed in space and did not include any model constructs to represent slippage. Several options were available to investigate if there were any valid points of comparison between the test and the model. At the time, this work was not continued due to budget limitations.

5.3.2 Restraint Layer Interface and Proofing

The restraint layer consists of the restraint bladder fabric and the webbing net, each of which has independent termination hardware. The restraint bladder fabric is finished in a deadman which rests in a notch in the interface ring. The bladder is sealed by a heat sealed flange which turns 90 degrees and uses a clamp ring and O-ring to seal. The sealing flange was formed in pieces using a vacuum forming process. To ensure that the flange would seal correctly a portion of the interface ring and clamp ring were printed on a stereolithography machine. An actual sample of the flange and fabric was then tested for a proper fit against the model. Figure 5.6 shows the model of the ring with a flange interface.

34
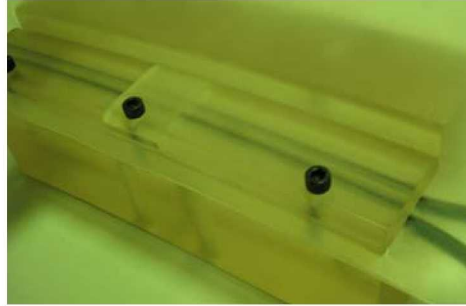
Figure 5.6. Restraint bladder interface test

The webbing subassembly was concurrently proof tested. Vectran webbing naturally has elongation in the fabric and it is important to stretch out the fibers when determining the final length. Each webbing was taken to 1.5 times the expected loading conditions in the fixture seen in Figure 5.7. This fixture uses the same pin used on the final configuration of the habitat interface.

Figure 5.7. Webbing proofing fixture

5.3.3 Small Scale Folding

The SOW required that the Thermal Micrometeoroid Cover layer mimic the thickness and folding characteristics of a flight TMC. While the exact design of a flight TMC is still a subject of research, a potential configuration was built at ILC in consultation with experts at ILC, LaRC, and JSC. The potential flight configuration is 2 inches in thickness and uses three layers of open cell foam as a Whipple bumper to break up Micrometeroids. The X-Hab TMC was built using more readily available and cost effective materials. These materials would never be flown but serve as a demonstration of a deployable TMC. The X-Hab TMC is also designed to block all UV light from hitting the Vectran to guarantee little to no degradation. Figure 5.8 is a photo comparing the two TMC configurations and their folding characteristics.

Figure 5.8. TMC comparison. Left is the flight and right is the demonstration TMC.

5.3.4 Interface Ring As-Built Testing

Photogrammetry was used to determine the accuracy of the bolt hole locations on the as-built interface rings. This technique uses a series of cameras to optically measure the 3D location of a target. To conduct the Photogrammetry, the natural dark cavities of the holes were used as markers for the hole locations. The rings' white paint resulted in a black target contrasted on a white background.

Vertical and horizontal 2721mm scale bars were set up in the field of view to calibrate the system but were found to be very hard to get a good scaling from. It was only possible to mark one of the scale bars for ring P/N 001. In this case we were able to set the scale for the end ring, but were not able to evaluate the experimental accuracy by calculating the length of a high accuracy scale bar. For ring P/N 002 post processing was not possible since neither scale bar could be marked. Figure 5.9 depicts the Photogrammetry test setup for the end rings and the calibration scale bars attached to the interface rings.

An attempt was made to locate the measured hole pattern relative to the design coordinates. These results are shown in Appendix E. for end ring P/N 001. With the chosen placement of the origin, the largest differences occurred near the bottom of the ring in quadrant 4.

There were several difficulties observed while post processing the experimental data. The scale bar targets ended up being too small and not in good focus. To overcome this and other difficulties that were experienced with the marking, the cameras should have been closer to the end ring for this experiment. This however would have required at least two additional camera angles. A retake was considered for the photogrammetry measurements, but was not acted on due to budget and delivery concerns.

When doing this work in the future we would not recommend using the dark shadow of the hole opening as the mark for machined holes. The shadow did not represent a hard fixed target in space, rather it represented the masking of the paint work, which in places was chipped and damaged. It is also not exactly clear where the shadow begins relative to the taper on the hole opening. By adding a designated target at each hole location, the accuracy of the measurement could be increased. This was not acted on due to budget and delivery deadlines.

ILC Dover plans to continue using Photogrammetry-based measurement on our inflatable softgoods products, at both desktop scales and for components larger than the end rings. For cases that fall into the category of more traditional hardware inspection of machined components, we would first consider other internal and external resources for the inspection or use the lessons learned in this program for more accurate measurements.

A second assessment of the hole locations of both interface rings was performed via a laser measurement system at Langley Research Center. This was used to compare with the results for P/N 001 listed in Appendix E. It was found that ILC's data was not accurate; therefore the laser measurements were used instead. The accuracy of the laser system was due in part to the inherently higher accuracy of laser over optical measurement and due to the use of targets that were screwed into the bolt holes.

36
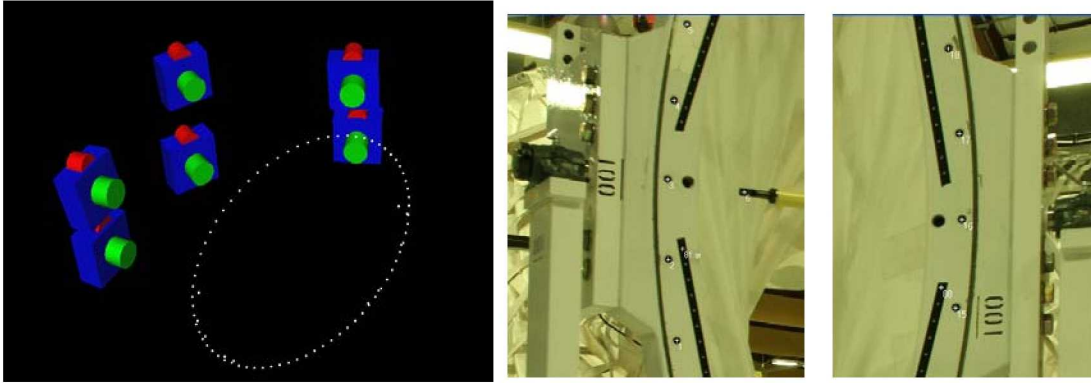
Figure 5.9. Interface ring test setup

6 Packing and Deployment

A crucial aspect of the X-Hab program is the packing and deployment procedure. Softgoods have the critical advantage of being able to pack in smaller launch vehicles and then expand upon delivery. This program hopes to demonstrate a softgood expansion that doubles the length of the habitat after deployment.

6.1 Deployment and Packing Plan

The deployment process can be accomplished through a mechanical system, gas inflation or a combination of both. To manage the softgoods during a mechanical deployment, a webbing mechanism using torsional springs for tension was designed that strung between the two interface rings. These deployment webbings ensure that the softgoods do not interfere with internal components and keeps them from falling to the ground as the rings separate. However, an inflation deployment may not need such a complex mechanism. Due to cost considerations, the deployment webbing mechanism was never built but could be applied in the future if desired. Figure 6.1 shows several images of a CAD model illustrating the deployment process.

Figure 6.1. Deployment Process

The packing procedure was based on several other programs at ILC and used a simple 'Z' folding technique. Packing rods on the inside of the interface rings provided a surface to pack and retain the folds. Other options for packing exist, however this is a straight forward approach and was deemed most suitable. It was determined that it would be advantageous to pack the softgoods on the inside of the endcaps to minimize stress on the fabric. In addition, packing the endcaps as close together as possible would allow the endcaps to be secured to one another and protect the softgoods during loading and launch. Based on the amount of material and the bend radius of the material, it was ascertained that the packing height would be approximately 3-4 inches. Figure 6.2 is a diagram of the pack height and bend radius of the material.
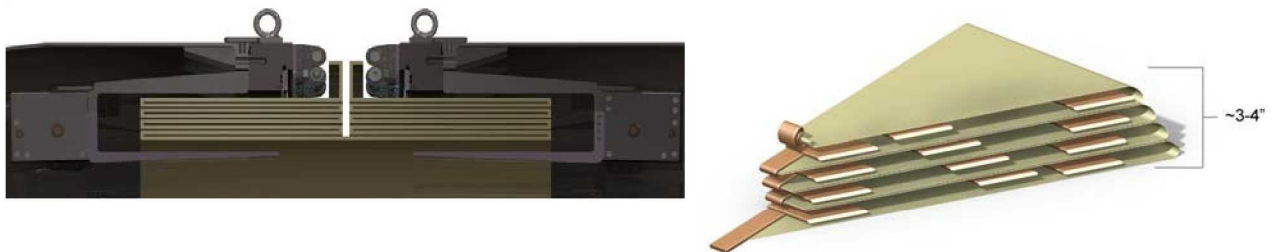

Figure 6.2. Packed State

6.2   Full Scale Packing

Several packing approaches were evaluated for this system. Two primary scenarios were examined: the 'Z' fold was the baseline and was evaluated against a random folding technique. . In both cases, the softgoods needed support to ensure proper packing and even material distribution. It was found that although it was efficient to pack a lot of material at the base of the packing rods and then to 'stretch' the material to pack the top, this caused an uneven deployment and stressed the fabric at the top. A sling underneath the softgoods at the 12 o'clock position was found to be sufficient support and was applied to both packing systems. The random folding technique involves putting material into the packing rods wherever it would allow. This method, although easy to employ, took up more volume than the 'Z' fold technique. Several iterations of the 'Z' folding were tested to eliminate the pulling and dragging of material on the floor. Simply staggering the folds produced the best results. However, this only had a minor effect on the deployment. Several designs were conceived to prevent too much fabric from falling out at one time but none were implemented due to cost concerns. Below was the optimal procedure determined for packing at ILC and Figure 6.3 illustrates the packing process.

- Moved both rings towards center allowing the softgoods to fall to the protected floor.
- Used overhead hoists to attach softgoods support strap.
- Supported windows from scaffolding to minimize stress on fabric.
- Used a staggered 'Z' fold technique on the softgoods. The first fold was pulled all the way to the back of the packing rod. Each of the subsequent folds was less than the previous fold to minimize pulling on the fabric during deployment. A total of three folds were used to pack each side with the window remaining in the center.
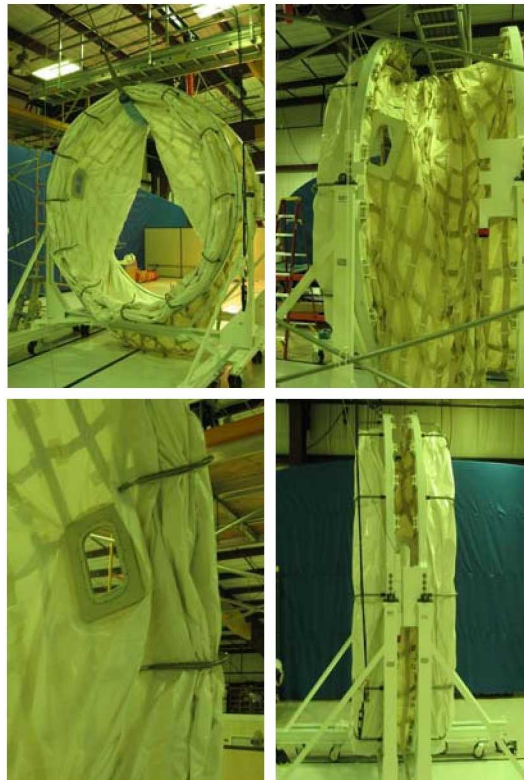- Pack second side and release window and softgood supports.

Figure 6.3. Packing at ILC

6.3 Full Scale Inflation Deployment

After evaluating mechanical and inflation deployments, the inflation deployment was demonstrated to require no more than 6 inches of water (.22 psi) for full deployment. This was an extremely efficient deployment approach that was easily repeatable in the lab. After each test, the X-hab was inspected for damage. The full scale deployment revealed several items that needed to be addressed on the final configuration. The parachute fabric endcaps were replaced with a more reliable sealing method and full Vectran endcaps since they were insufficient for pressures greater than 3 inches of water. The more reliable sealing method used a plastic, water jet cut clamp ring that aligned with the 72 bolt holes on each interface ring. Also the hoop webbings closest to the interface rings pulled down on the axial webbings, popping the indexing tabs off. To mitigate this concern the last hoop webbings by each ring were placed under the axial webbings. Initial inflation testing also revealed the need for greater indexing on the webbing net due to slippage and movement between the longitudinal and hoop straps. Hand tacking was used at the crossovers for superior control of the webbing upon deployment. The acceptance test report can be found in Appendix E. Figure 6.4 shows one of the later deployment tests with the Vectran endcaps and tacked webbing net.
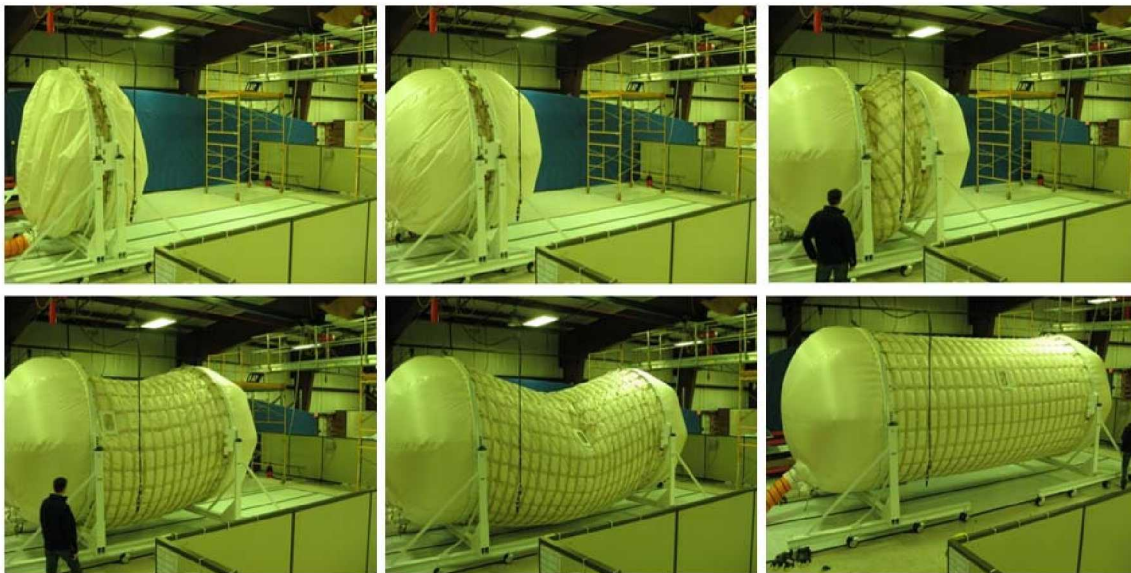
Figure 6.4. Deployment at ILC

6.4 TMC Packing and Integration

Packing the Thermal Micrometeoroid Cover begins by laying it out as flat as possible. The TMC is then folded inward, symmetrically, with two folds on each side. Then, the TMC is picked up and laid over the top of the packed habitat. The d-rings along the long edges of the TMC are then laced together, shoelace style, from one end to the other, then secured. A flap is placed over the laced cord for protection upon deployment. The TMC layer is interfaced with the end rings using a deadman system. A cord is simply belted around the end rings to secure the softgoods at the deadman location on the endcaps. The TMC deploys automatically as part of the habitat deployment. After the habitat is completely deployed, secondary tightening of the lacing is required. Figure 6.5 is a photograph of the actual demonstration TMC layer laid out flat and Figure 6.6 shows the conceptual integration of the TMC layer with the EDU. Figure 6.7 depicts the conceptual lacing configuration of the TMC layer. Nomex cord was included with the final

delivery of the unit. Onsite testing of the lacing will need to occur to determine the optimal lacing procedure.

Figure 6.5. Demonstration TMC for X-Hab
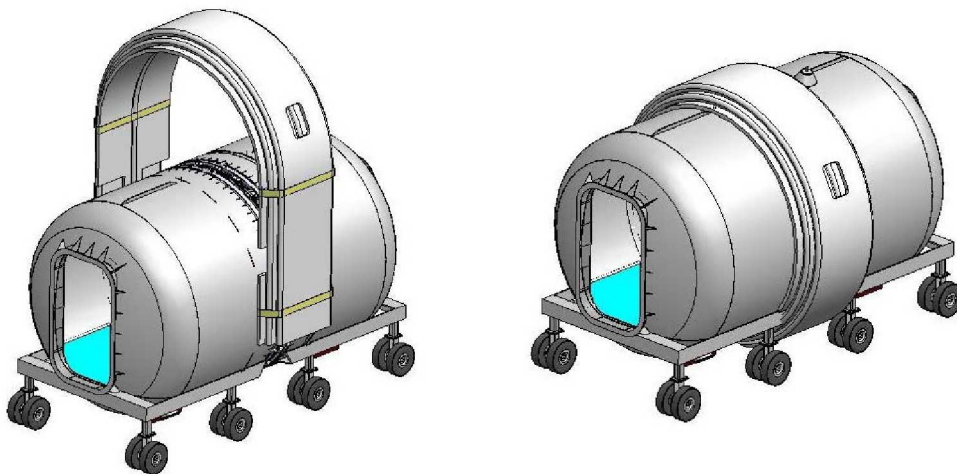
Figure 6.6. Integration of TMC

Figure 6.7. Lacing of TMC

7   Master Equipment List

A Master Equipment List (MEL), was assembled to track parts and masses of the components. The parts that were tracked on the MEL were those provided by ILC that were expected to be used on the final system. The list is color coded where yellow is the entire system and blue is the total for the major subsystems. The list is broken into three columns: units per assembly, assemblies per system, and units per system. In general the assembly refers to one interface 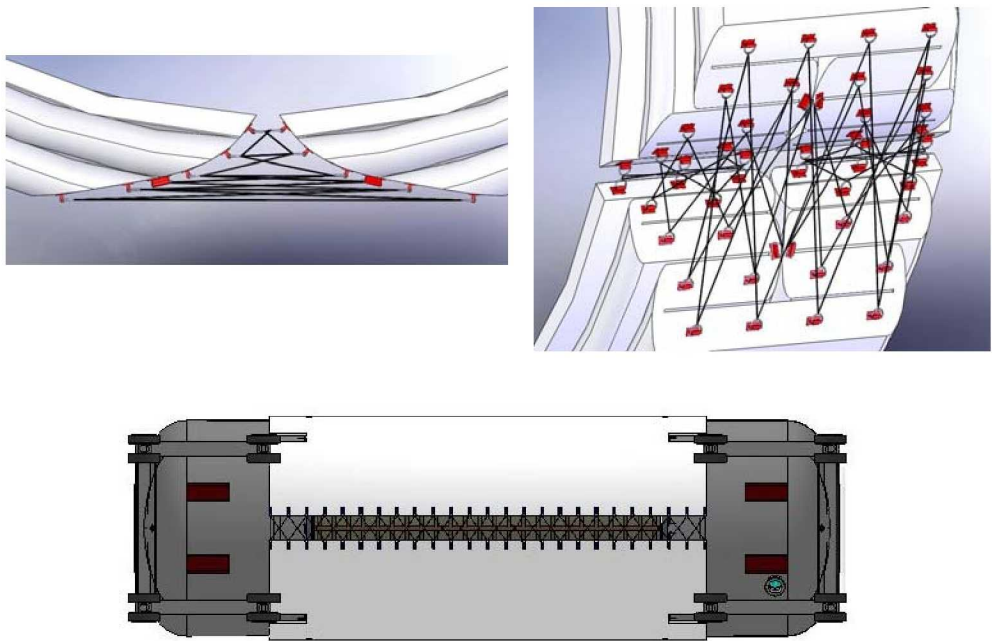ring. The units per assembly are generally how many units correspond to the interface ring and the units per system is the global quantity of units. The ILC supplied configuration has a total estimated weight of 3367.28 lbs. This weight is based on weights, solid models, supplier information, and engineering estimates. Table 7.1 is a summary of the MEL while Appendix C lists the complete MEL.

Table 7.1. Master Equipment List Summary

Item Information:							Mass Estimate (lbs):			
Line No.	Item	Material	Comment	Units per Assembly	Assembly's per System	Units per System	Unit	Assembly	System	Basis of Estimate
1	X-Hab Lunar Module								3367.28	
2	Ring Assembly						1022.99	1080.63	2102.73	
12	Axial Webbing Bracket						2.49	70.90	141.80	
19	Deployment System						2.21	26.52	53.04	
21	Floor						156.86	642.18	642.18	
25	Window						12.12	13.56	27.12	
34	Restraint Softgoods						35.13	110.00	110.00	
40	TMC						145.25	145.25	290.41	

8   Notables and Lessons Learned

There were several important lessons learned during the course of this program. Perhaps the most important is that only minimal subscale testing is applicable to a full test unit. The packing and deployment plans were valuable as baselines when it came to packing and deploying the full scale version. Scaling was an especially prevalent issue in replicating a single fabric lobe for testing. With several more iterations it is believed that a robust fixture that fully mimicked the webbing and the needed movement could be created. However, time and budget restraints had to be considered.

A promising outcome of the program was the ability to manufacture softgoods components within tight tolerances. This can be seen in the critical component of the axial webbings. The design of the webbing fixture and proofing procedure reduced the error in the length of the webbings to .375 inches. This small error was reduced by using shims on the axial webbing bracket. Future programs can use similar practices and hopefully continue to reduce the manufacturing tolerance.

A lesson learned in the program was that the 'sleaziness', or the ability for the webbing to rack or skew, plays a significant role in the final configuration. Throughout the program several steps were taken to ensure that even though the webbing straps were not tied together, the maximum opening allowed by the webbing would still provide a safety factor of 4 on the restraint layer. In the end, it was not the opening of the webbings that caused a problem but that the hoop webbings were rotating about the axis perpendicular to the length of the habitat creating a 'bowing' effect in the back of the structure due to the initial sag of the softgoods under gravity. After careful consideration, hand tacking of the webbing was used to create a net and reduce the movement of the webbing during deployment. This solved the problem and allowed the habitat to deploy to its' designed shape with more even fabric distribution.

Photogrammetry was attempted to determine the accuracy of the hole locations in the interface rings. Photogrammetry is a powerful tool, but the setup approach and time required for accurate measurements needs to be well researched to produce useful measurements and the limitations of the system must be well understood.

This program established new manufacturing and design techniques that will be applied to future applications. One of those design techniques that will serve the community well in the future is the analysis of the webbings and the single fabric lobe structure. The analysis established our baseline tolerances and determined the required over-sizing in the fabric. These were critical aspects that were iterated with the design team to find the optimal solution.

9   Conclusion

The EDU will be used to evaluate important research questions such as hybrid structure integration, softgoods packaging and deployment, and interior outfitting. The structure is designed for reconfiguration and future modification to demonstrate testing of ideas that are currently only conceptual. The current EDU is designed to allow integration of a deployable floor with minimal impact on the current system. Testing at the full pressure of 9 psi will answer many engineering and manufacturing questions. A certification plan could also be developed, allowing this unit to set a precedent for acceptance of all future expandable habitat systems.

The X-Hab is an Engineering Development Unit meant to further the design and acceptability of softgood engineered expandable habitats. The benefits of an expandable design are significant. This unit is designed as a test bed to answer questions from supporters and critics alike as the United States looks beyond low earth orbit.

10 Appendix A: References

Cadogan, D.P., Scheir, C., Dixit, A., "Intelligent Materials for Deployable Space Structures (InFlex)", 2006-01-2065, 36th International Conference on Environmental Systems, Norfolk VA, 20-27 July, 2006.

Cadogan, D.P., Scheir, C., "Expandable Habitat Technology Demonstration for Lunar and Antarctic Applications", 2008-01-2024, International Conference on Environmental Systems, San Francisco CA ,29 June – 2 July 2008.

D. Cadogan, C. Sandy, M. Grahne, "Development and Evaluation of the Mars Pathfinder Inflatable

Airbag Landing System", 49th International Astronautical Congress Paper No. IAF-98-I.6.02, September 28 - October 2, 1998, Melbourne, Australia.

Kennedy, Kriss (2002). "Lessons from TransHab: An Architect's Experience". *AIAA Space Architecture Symposium*. AIAA 2002-6105.

Kennedy, Kriss J., "TransHab and the Space Architects", *Fabric Architecture*, published Sept.-Oct. 1999, pp. 24-30, 48-50.

Kennedy, Kriss J., "Inflatable Habitat Structure", NASA MSC-22029, July 5, 1993.

D. Cadogan, J. Stein, T. Fredrickson, G. Sharpe, "Deployable Lunar Habitat Design and Materials Study," Phase I Program Technical Report, January 29, 1997, NASA JSC.

Brown, Mariann F. and Schentrup, Susan M., "Requirements for Extravehicular Activities on the Lunar and Martian Surfaces," *SAE Technical Paper Series*, 901427, 1990.

Simonsen, Lisa C., Nealy, John E., "Radiation Protection for Human Missions to the Moon and Mars", NASA Technical Paper 3079, February 1991.

Rais-Rohani, M. "On Structural Design of a Mobile Lunar Habitat With Multi-Layered Environmental Shielding", NASA/CR—2005–213845.

Dorsey, J. T., Wu, K. C., Smith, R. "Structural Definition and Mass Estimation of Lunar Surface Habitats for the Lunar Architecture Team Phase 2 (LAT-2) Study", *Earth and Space Conference 2008,* Long Beach, CA, 2008.

Ware, "Evaluation of Flammability Standards and Test Methodologies for Applicability to the Expandable Lunar Module Test Unit", *ILC Dover, LP*, 16 July 2008

11 Appendix B: Acronyms

EDU	Engineering Development Unit
EVA	Extra Vehicular Activity
FEA	Finite Element Analysis
Fed Std	Federal Standard
FEM	Finite Element Model
FR	Flame Retardant
ILC	ILC Dover, LP
InFlex	Intelligent Flexible Material Program
LaRC	Langley Research Center
LAT	Lunar Architecture Team
MLI	Multi Layer Insulation
MMOD	MicroMeteoroid and Orbital Debris
MMSE	MicroMeteoroid and System Ejecta
NASA	National Aeronautics and Space Administration
psi	pounds per square inch
psig	pounds per square inch gage (interchangeable with psi)
TMC	Thermal Micrometeoroid Cover
TTS	Time Temperature Superposition
UTS	Ultimate Tensile Strength
X-Hab	Expandable Habitat

12 Appendix C: Master Equipment List

Line No.	Item	Material	Comment	Units per Assembly	Assembly's per System	Units per System	Unit	Assembly	System	Basis of Estimate
Item Information:							Mass Estimate (lbs):			
1	X-Hab Lunar Module								3367.28	
2	Ring Assembly						1022.99	1080.63	2102.73	
3	Base Ring	A36 Steel	Paint	1	2	2	1001.70	1001.70	2003.40	Solid Model Calculation
4	Clamp Ring	Aluminum 6061-T6	Clear Anodized	3	2	6	6.12	18.36	36.72	Solid Model Calculation
5	Clamp Ring Screws	Stainless Steel	14-20 x 5/8 90910A540	120	2	240	0.01	1.24	2.47	McMaster
6	Locating Plate	4140 Steel	Powder Coated	3	1	3	0.57	1.72	1.72	Solid Model Calculation
7	Locating Plate Screws	Stainless Steel	3/8"-16 x 7/8" PN: 92949A623	6	1	6	0.04	0.22	0.22	Solid Model Calculation/McMaster
8	Eye-Bolt Top	Steel	5/8"-11 PN: 3049T93	2	2	4	0.40	0.80	1.60	Solid Model Calculation/McMaster
9	Eye-Bolt Inside	Steel	1/2"-13	2	2	4	-	-	-	LaRC (ILC order)
10	Backside Bolt	Steel	1/2-13 x 1.231" PN: 92620A713	72	2	144	-	-	-	LaRC (ILC order)
11	Spacer Plate	4140 Steel	Powder Coated	4	1	4	14.15	56.60	56.60	Solid Model Calculation
12	Axial Webbing Bracket						2.49	70.90	141.80	
13	Bracket	4140 Steel	Powder Coated	26	2	52	1.64	42.74	85.49	Solid Model Calculation
14	Shoulder Bolt	18-8 Stainless Steel	3/4" x 3-1/4" PN: 90298A848	26	2	52	0.56	14.51	29.02	Solid Model Calculation/McMaster
15	Nut	Steel	5/8"-11 PN:94846A533	26	2	52	0.05	1.35	2.70	Solid Model Calculation/McMaster
16	Washer	18-8 Stainless Steel	3/4" PN: 98017A220	52	2	104	0.02	1.04	2.08	Solid Model Calculation/McMaster
17	Securing Bolt	Steel	9/16"-12 PN: 92620A765	52	2	104	0.20	10.22	20.44	Solid Model Calculation/McMaster
18	Shim	Washer	t=.125" PN: 98126A840	52	2	104	0.02	1.04	2.08	McMaster
19	Deployment System						2.21	26.52	53.04	
20	Packing Rod	Stainless Steel	Uses concentric lock	12	2	24	2.21	26.52	53.04	Solid Model Calculation
21	Floor						156.86	642.18	642.18	
22	Floor Beam	Aluminum 6061-T6	Machined	3	1	3	119.90	359.70	359.70	Sized Part
23	Floor Panel, 56"	Fiberglass grating	Fibergrate	8	1	8	33.66	269.28	269.28	Purchased Part
24	Floor Panel, 5"	Fiberglass grating	Fibergrate	4	1	4	3.30	13.20	13.20	Purchased Part
25	Window						12.12	13.56	27.12	
26	Window Frame	Aluminum 6061-T6	Churchman's Machining	1	2	2	5.81	5.81	11.62	Solid Model Calculation
27	Webbing Plate	Aluminum 6061-T6	Churchman's Machining	1	2	2	1.69	1.69	3.39	Solid Model Calculation
28	Inner Pane Plate	Aluminum 6061-T6	Churchman's Machining	1	2	2	0.97	0.97	1.94	Solid Model Calculation
29	Deadman Plate	Aluminum 6061-T6	Churchman's Machining	1	2	2	2.56	2.56	5.13	Solid Model Calculation
30	Window Pane	Polycarbonate	Space Suit Bubble Material	1	2	2	0.97	0.97	1.94	Solid Model Calculation
31	Inner Pane Screws	Steel	McMaster	16	2	32	0.04	0.69	1.38	Solid Model Calculation
32	Deadman Plate Screws	Steel	McMaster	12	2	24	0.04	0.44	0.89	Solid Model Calculation
33	Webbing Plate Screws	Steel	McMaster	10	2	20	0.04	0.43	0.85	Solid Model Calculation
34	Restraint Softgoods						35.13	110.00	110.00	
35	Restraint Fabric	200 denier Vectran	Urethane coated with FR additive	1	1	1	32.00	32.00	32.00	Weighed
36	Axial Index Tab	Velcro and 200 denier Vectran	Weight in Restraint Fabric	299	1	299	0.00	0.00	0.00	Weighed
37	Hoop Index Tab	Velcro and 200 denier Vectran	Weight in Restraint Fabric	324	1	324	0.00	0.00	0.00	Weighed
38	Axial Webbing	24k Vectran	Includes sewing	26	1	26	1.50	39.00	39.00	Weighed
39	Hoop Webbing	24k Vectran	Includes sewing	24	1	24	1.63	39.00	39.00	Weighed
40	TMC						145.25	145.25	290.41	
41	Outer Protective Layer	FR Nomex	Includes flap and 12" overalp	1	1	1	24.10	24.10	24.10	Engineering Estimate
42	Insulation	Thinsulate	1 layer	1	1	1	31.49	31.49	31.49	Engineering Estimate
43	Whipple Bumper	Foam and Poly	3 layers	1	3	3	72.58	72.58	217.74	Engineering Estimate
44	Inner Layer	Polyester	Includes lacing strip	1	1	1	17.08	17.08	17.08	Engineering Estimate

13 Appendix D: Webbing Seam Data

As sewn seam testing

TEST REPORT

Metallurgical Engineering and Testing
51229 Century Court
Wixom, MI 48393-2074 USA

Contact: Lauren Shook
ILC DOVER
ONE MOONWALKER ROAD
Frederica, DE 19946-2080

Telephone: (248) 960-4900
Telefax : (248) 960-5966
Website : www.storksmt.com/crs

Purchase Order No. : 294676		**Report No.**	: ILC006-08-10-17132-1
Date Received : 10/6/2008		**Report Date**	: 10/13/2008
Report Delivered Via: ShookL@ILCDover.com			
Attachments : Load vs Position Graphs			

Work Requested: Pull Testing of 2" Wide Webbing. Nine (9) Samples.

SCRS ID	Customer ID:
1	1
2	2
3	3
4	4
5	5
6	6
7	7
8	8
9	9

Mechanical Testing Results

SCRS ID	Peak Load (lbf)	Peak Load (kn)
1	37,380	166.3
2	39,570	176.0
3	39,280	174.7
4	37,470	166.7
5	39,160	174.2
6	37,050	164.8
7	44,960	200.0
8	40,510	180.2
9	43,300	192.6
Methods	CUST	CUST

Method(s)
- CUST – Testing performed per instructions from customer.

Respectfully submitted

John Alexander (248) 960-4900 Ext: 453

Stork Climax Research Services, Inc.

─Load vs Position─

42000

37800   00006784
             10-13-2008
33600   01:11:04 PM

29400

25200

31000 (Lbs)

16800

12600

8400

4200   Customer: ILC DOVER
             Job Number: 17132
             Specimen: 01
0   COMMENTS:

0.000 0.160 0.320 0.480 0.640 0.800 0.960 1.120 1.280 1.440 1.600
                              (In)

50
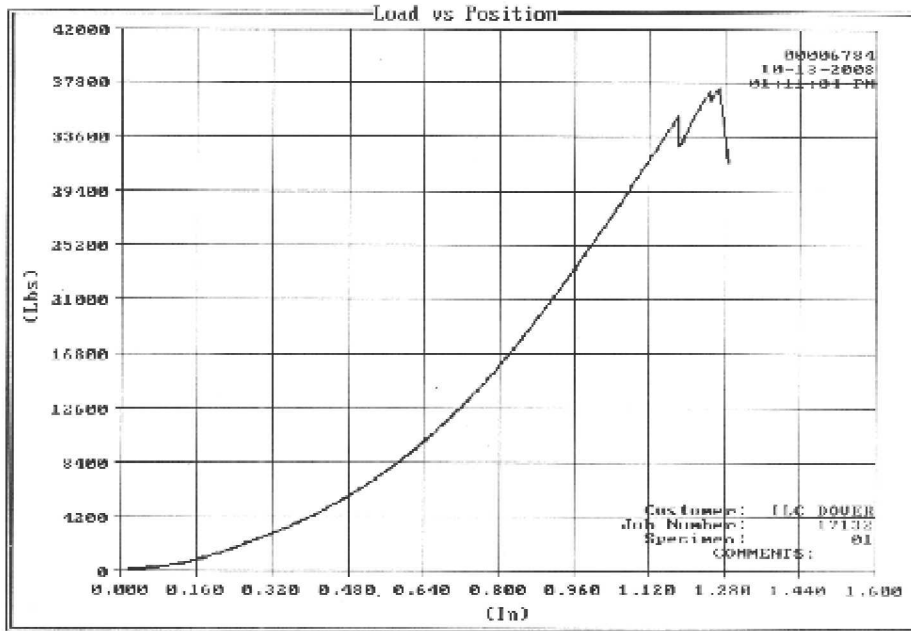
Alternate seam configuration testing

Stork Climax Research Services, Inc.

TEST REPORT

Contact: Lauren Shook
ILC DOVER
ONE MOONWALKER ROAD
Frederica, DE 19946-2080

Metallurgical Engineering and Testing
51229 Century Court
Wixom, MI 48393-2074 USA

Telephone: (248) 960-4900
Telefax : (248) 960-5966
Website : www.storksmt.com/crs

Purchase Order No. : 294639		**Report No.**	: ILC006-08-08-16034-1
Date Received : 8/27/2008		**Report Date**	: 8/29/2008
Report Delivered Via : shookl@ILCDover.com			
Attachments : Load vs Position Graphs			

Work Requested: Pull Testing of 2" Wide Webbing. Ten (10) Samples.

SCRS ID	Customer ID:
1	1
2	1
3	2
4	2
5	3
6	3
7	4
8	4
9	5
10	5

Mechanical Testing Results

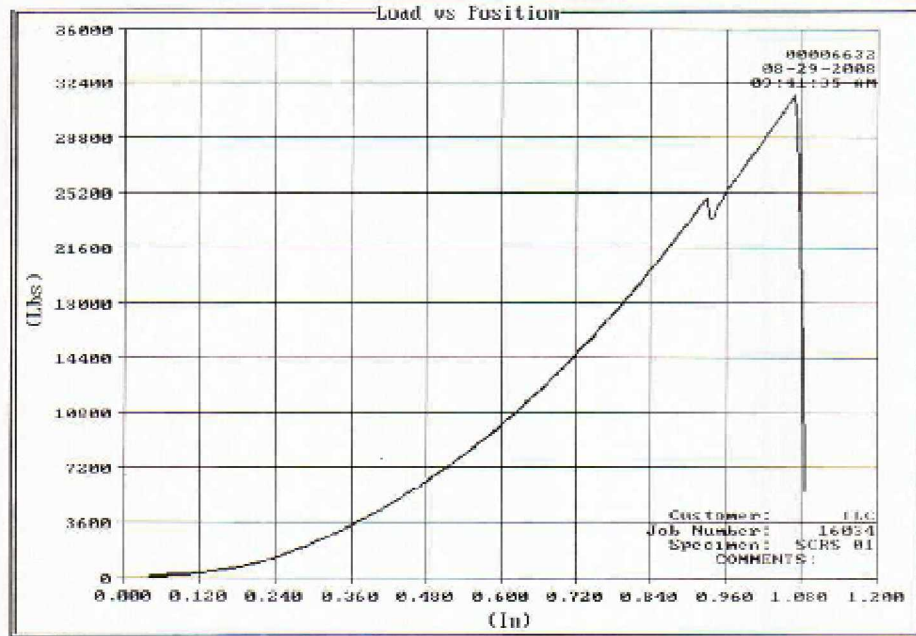| SCRS ID	Peak Load (lbf)	Peak Load (kn)
1	31,600	140.6
2	30,600	136.1
3	34,300	152.6
4	34,700	154.4
5	32,500	144.6
6	41,600	185.0
7	36,800	163.7
8	32,600	145.0
9	32,200	143.2
10	30,400	135.2
Methods	*CUST*	*CUST*

All specimens broke at the lap stiching.

Method(s)
• CUST – Testing performed per instructions from customer.

Respectfully submitted

[signature]

Dennis Galloway (248) 960-4900 Ext: 456

Page 1 of 1

14 Appendix E: Photogrammetry Data

Interface Ring Testing

Quadrant 1

x Design	x Measured	y Design	y Measured
59.	58.9949	0.	4.26' 10^{-14}
58.7755	58.7624	5.14219	5.12619
58.1037	58.0836	10.2452	10.2317
56.9896	56.9875	15.2703	15.2638
55.4419	55.4211	20.1792	20.1647
53.4722	53.4532	24.9345	24.9164
51.0955	51.0844	29.5	29.4832
48.33	48.3086	33.841	33.8277
45.1966	45.1789	37.9245	37.9132
41.7193	41.6951	41.7193	41.7083
37.9245	37.9002	45.1966	45.1903
33.841	33.8223	48.33	48.3242
29.5	29.4888	51.0955	51.0963
24.9345	24.9135	53.4722	53.4895
20.1792	20.1644	55.4419	55.4613
15.2703	15.2526	56.9896	57.0153
10.2452	10.2254	58.1037	58.1251
5.14219	5.13497	58.7755	58.7923

Quadrant 2

x Design	x Measured	y Design	y Measured
0.	-0.0184119	59.	59.0006
-5.14219	-5.16987	58.7755	58.7969
-10.2452	-10.261	58.1037	58.1118
-15.2703	-15.2915	56.9896	56.995
-20.1792	-20.1949	55.4419	55.45
-24.9345	-24.938	53.4722	53.4738
-29.5	-29.504	51.0955	51.0888
-33.841	-33.8397	48.33	48.3202
-37.9245	-37.9282	45.1966	45.1947
-41.7193	-41.7271	41.7193	41.7114
-45.1966	-45.1853	37.9245	37.9186
-48.33	-48.3198	33.841	33.8241
-51.0955	-51.0878	29.5	29.4834
-53.4722	-53.458	24.9345	24.9314
-55.4419	-55.4151	20.1792	20.1631
-56.9896	-56.9843	15.2703	15.2546
-58.1037	-58.1009	10.2452	10.2335
-58.7755	-58.7674	5.14219	5.15004

Quadrant 3

x Design	x Measured	y Design	y Measured
-59.	-58.9949	0.	4.26' 10^{-14}
-58.7755	-58.7914	-5.14219	-5.13465
-58.1037	-58.1196	-10.2452	-10.2367
-56.9896	-57.0243	-15.2703	-15.2583
-55.4419	-55.475	-20.1792	-20.1662
-53.4722	-53.5052	-24.9345	-24.9304
-51.0955	-51.1475	-29.5	-29.4977
-48.33	-48.3829	-33.841	-33.8446
-45.1966	-45.2443	-37.9245	-37.9311
-41.7193	-41.7794	-41.7193	-41.7414
-37.9245	-37.9832	-45.1966	-45.2135
-33.841	-33.8989	-48.33	-48.3536
-29.5	-29.5554	-51.0955	-51.1159
-24.9345	-24.9908	-53.4722	-53.5194
-20.1792	-20.2306	-55.4419	-55.4924
-15.2703	-15.323	-56.9896	-57.0454
-10.2452	-10.2966	-58.1037	-58.1616
-5.14219	-5.18589	-58.7755	-58.8355

Quadrant 4

x Design	x Measured	y Design	y Measured
0.	-0.0394526	-59.	-59.0689
5.14219	5.10944	-58.7755	-58.856
10.2452	10.2285	-58.1037	-58.1751
15.2703	15.2475	-56.9896	-57.0718
20.1792	20.1745	-55.4419	-55.5191
24.9345	24.9255	-53.4722	-53.5487
29.5	29.5075	-51.0955	-51.1562
33.841	33.854	-48.33	-48.3963
37.9245	37.9461	-45.1966	-45.2473
41.7193	41.7417	-41.7193	-41.767
45.1966	45.2185	-37.9245	-37.9628
48.33	48.3562	-33.841	-33.8765
51.0955	51.1096	-29.5	-29.5352
53.4722	53.4864	-24.9345	-24.9579
55.4419	55.4637	-20.1792	-20.208
56.9896	56.9901	-15.2703	-15.288
58.1037	58.1106	-10.2452	-10.2576
58.7755	58.7679	-5.14219	-5.15316

REPORT DOCUMENTATION PAGE

1. REPORT DATE *(DD-MM-YYYY)*	2. REPORT TYPE	3. DATES COVERED *(From - To)*
01-03-2010	Contractor Report	

4. TITLE AND SUBTITLE

Intelligent Flexible Materials for Space Structures - Expandable Habitat Engineering Development Unit

5a. CONTRACT NUMBER

NNL05AA28C

5b. GRANT NUMBER

5c. PROGRAM ELEMENT NUMBER

6. AUTHOR(S)

Hinkle, Jon; Sharpe, George; Lin, John; Wiley, Cliff; Timmers, Richard

5d. PROJECT NUMBER

5e. TASK NUMBER

5f. WORK UNIT NUMBER

441261.01.04

7. PERFORMING ORGANIZATION NAME(S) AND ADDRESS(ES)

NASA Langley Research Center
Hampton, VA 23681-2199

8. PERFORMING ORGANIZATION REPORT NUMBER

9. SPONSORING/MONITORING AGENCY NAME(S) AND ADDRESS(ES)

National Aeronautics and Space Administration
Washington, DC 20546-0001

10. SPONSOR/MONITOR'S ACRONYM(S)

NASA

11. SPONSOR/MONITOR'S REPORT NUMBER(S)

NASA/CR-2010-216682

12. DISTRIBUTION/AVAILABILITY STATEMENT

Unclassified - Unlimited
Subject Category 39
Availability: NASA CASI (443) 757-5802

13. SUPPLEMENTARY NOTES

Langley Technical Monitor: Thomas C. Jones

14. ABSTRACT

Expandable habitable elements are an enabling technology for human exploration in space and on planetary surfaces. Large geometries can be deployed from a small launch volume, allowing greater mission capability while reducing mass and improving robustness over traditional rigid shells. This report describes research performed by ILC Dover under the Intelligent Flexible Materials for Space Structures program on the design and manufacture of softgoods for LaRC's Expandable Habitat Engineering Development Unit (EDU). The EDU is a full-scale structural test article of an expandable hybrid habitat, integrating an expandable softgoods center section with two rigid end caps. The design of the bladder, restraint layer and a mock-up Thermal Micrometeoroid Cover is detailed together with the design of the interface hardware used to attach them to the end caps. The integration and design of two windows and a floor are also covered. Analysis was performed to study the effects of the open weave design, and to determine the correct webbing and fabric configuration. Stress analyses were also carried out on the interfaces between the softgoods and the end caps and windows. Testing experimentally determined the strength of the fabric and straps, and component testing was used to proof several critical parts of the design. This program established new manufacturing and design techniques that can be applied to future applications in expandable structures.

15. SUBJECT TERMS

Expandable structures; Inflatables; Softgoods; Habitats; Packaging; Deployment; Surface Systems; Hybrid; Engineering Development Unit; EDU

16. SECURITY CLASSIFICATION OF:			17. LIMITATION OF ABSTRACT	18. NUMBER OF PAGES	19a. NAME OF RESPONSIBLE PERSON
a. REPORT	b. ABSTRACT	c. THIS PAGE			STI Help Desk (email: help@sti.nasa.gov)
U	U	U	UU	56	19b. TELEPHONE NUMBER *(Include area code)* (443) 757-5802